IX Winter School on Theoretical Physics
NONLINEAR PHENOMENA IN CONDENSED MATTER

January 30 - February 6, 2011, Dubna, Russia

ТЕОРЕТИЧЕСКИЕ МОДЕЛИ ВНУТРЕННИХ ДЖОЗЕФСОНОВСКИХ ПЕРЕХОДОВ В СЛОИСТЫХ СВЕРХПРОВОДНИКАХ

Шукринов Ю. М. (ЛТФ, ОИЯИ)

Краткое содержание

- 1.1. Модель ССДП с емкостной связью.
- - Обобщенное соотношение Джозефсона и система уравнений для СДП
- - Методика расчета

1.2. CCJJ модель с диффузионным током (CCJJ+DC модель)

- 1.3. Параметрический резонанс

Layered $Bi_2Sr_2CaCu_2O_y$(Bi2212) single crystals represent natural stacks of atomic scale intrinsic Josephson junctions.

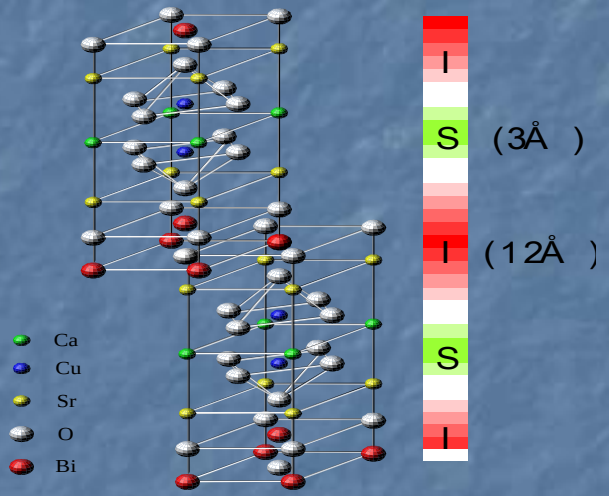

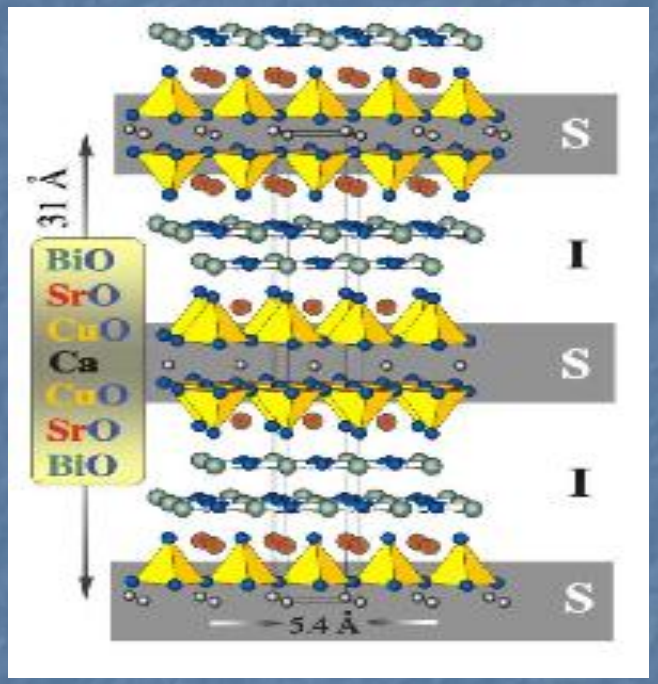

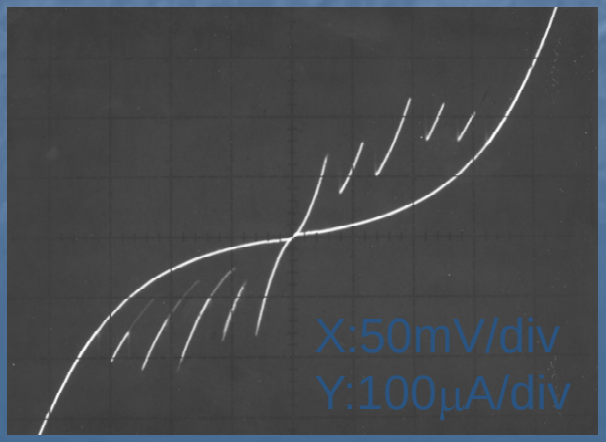

I-V characteristics

- Multi-branch structure
- large hysteresis
- Roughly equal spacing

Experimental IVC of BSCCO-2212 (Sample Ea, 10K; Eb, 35K) :Kyoto university, Japan

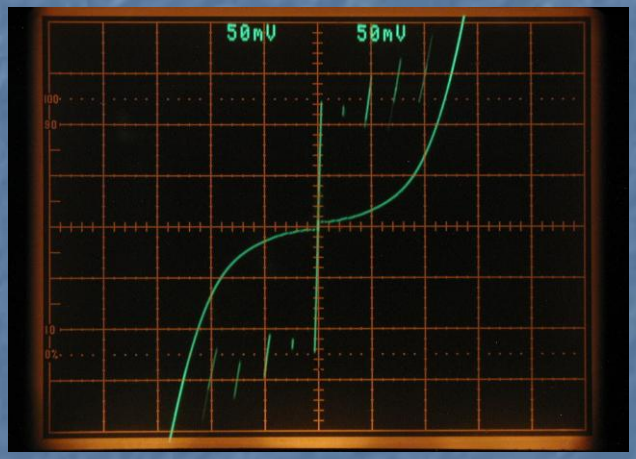

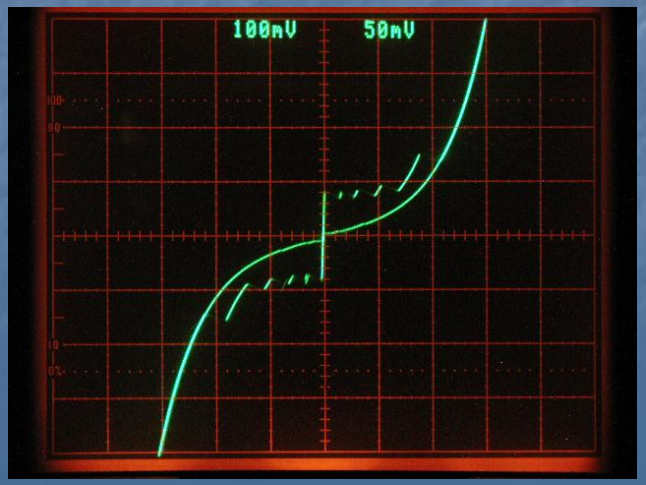

R.Kleiner, P.Muller, 1992

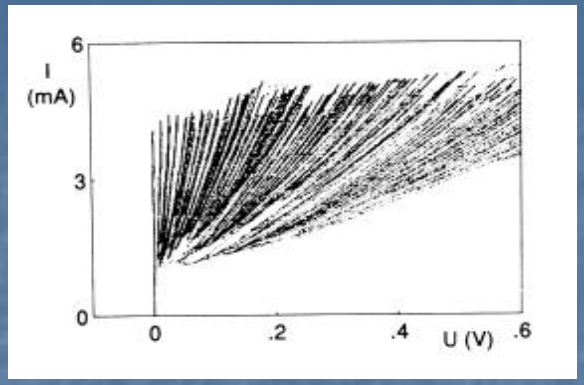

Experimental IVC of BSCCO-2212 (Sample #1) K.Okanoue, K.Hamasaki, APL, 87,222506, (2005)

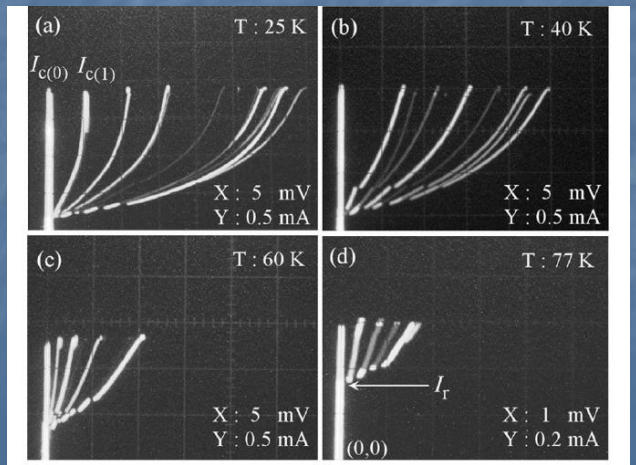

FIG. 2. *I-V* characteristics of a self-planarized stack (Sample No. 1) at 25, 40, 60, and 77 K.

Субщелевая структура на ВАХ

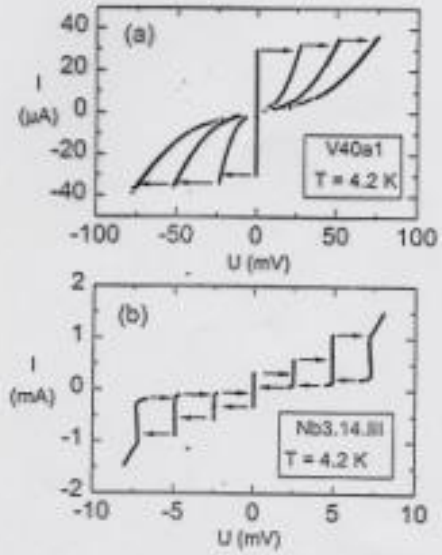

FIG. 2. (a) First three branches of the *I-V* characteristic of a $Tl_2Ba_2Ca_2Cu_3O_{10+\delta}$ step stack with a total number of 130 junctions; (b) *I-V* characteristics of an artificial three-junction Nb/Al-AlO_x/Nb stack. Arrows indicate voltage switching.

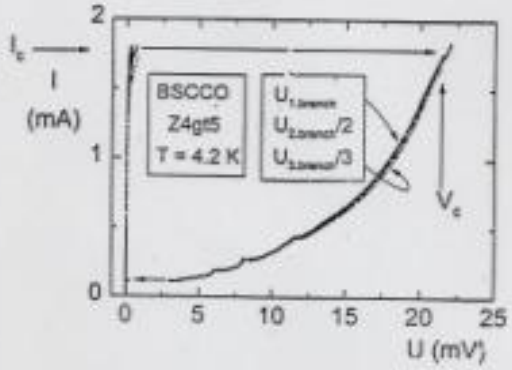

FIG. 3. Comparison of the first three branches of the *I-V* characteristic of a BSCCO mesa. The voltages of the second (third) branch have been divided by two (three).

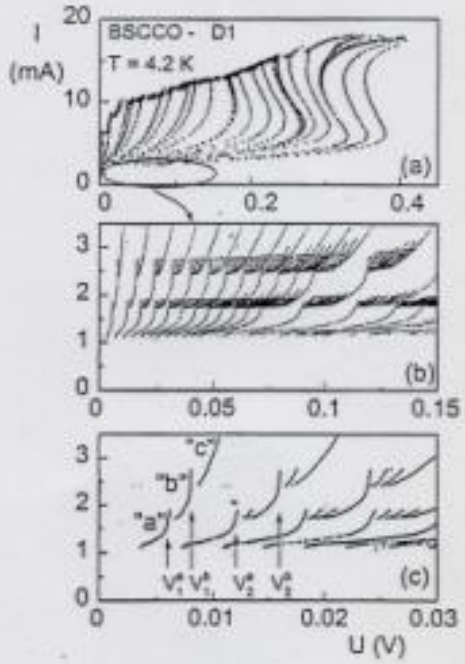

FIG. 10. (a) *I-V* characteristic of a BSCCO mesa at $T = 4.2$ K. Not all branches are traced out. With increasing number of resistive junctions, heating effects cause a backbending of the *I-V* curve. (b) Enlargement of the region indicated in (a) showing the extremely regular structures in all branches. (c) The same data on an expan scale with the sub-branch- *a*, *b*, and *c* and the structure vo V_1^a, V_1^b, V_2^a, and V_2^b marked.

APPLIED PHYSICS

Filling the Terahertz Gap

Reinhold Kleiner

A device made from a layered superconductor emits electromagnetic waves in a frequency range for which good radiation sources had been lacking.

At almost every frequency, we have good methods to generate and detect electromagnetic radiation. One crucial exception is the low terahertz range, where despite intensive research there is a severe lack of devices such as oscillators and detectors. With better terahertz technology, researchers could develop new kinds of nondestructive imaging for materials testing and medical diagnosis, and carry out novel spectroscopic studies of materials and molecules.

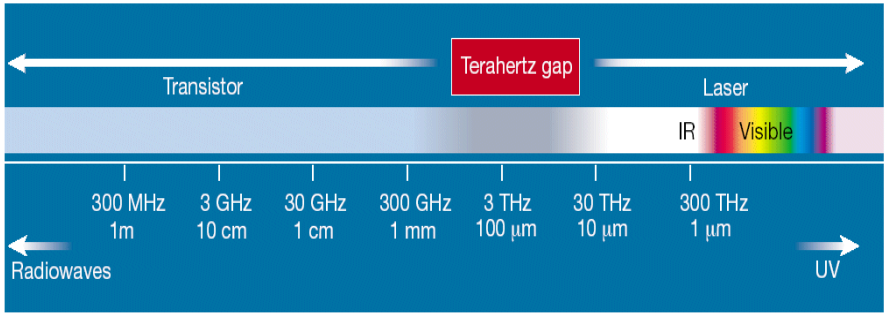

Figure 1 The terahertz gap. The gap, lying roughly between 300 GHz (0.3 THz) and 30 THz, exists because the frequencies generated by transistors and lasers, typical semiconductor devices, don't overlap. No current semiconductor technology can efficiently convert electrical power into electromagnetism in that range. But the 'heterostructure laser' produced by Köhler *et al.*[1] might, in due course, meet the demand for radiation sources at these terahertz wavelengths.

Emission of Coherent THz Radiation from Superconductors

L. Ozyuzer,[1,2] A. E. Koshelev,[2] C. Kurter,[2,3] N. Gopalsami,[4] Q. Li,[2] M. Tachiki,[5] K. Kadowaki,[6] T. Yamamoto,[6] H. Minami,[6] H. Yamaguchi,[6] T. Tachiki,[7] K. E. Gray,[2] W.-K. Kwok,[2] U. Welp[2]*

Emission of Coherent THz Radiation from Superconductors (1)
23 NOVEMBER 2007 VOL 318 SCIENCE

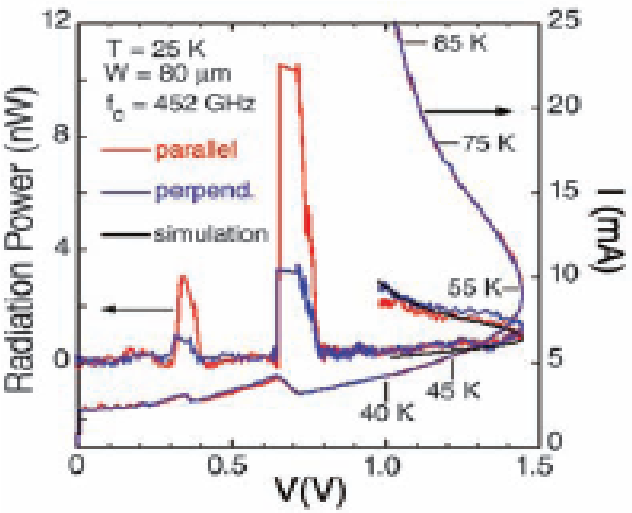

Fig. 2. Current-voltage characteristics and radiation power of the 80-μm mesa. The voltage dependence of the current (right *y*-axis) and of the radiation power (left *y*-axis) at 2.5 K for parallel and perpendicular settings of the filter with 0.452 THz cut-off frequency are shown for decreasing bias in zero applied magnetic field. Polarized Josephson emission occurs near 0.71 and 0.37 V, and unpolarized thermal radiation occurs at higher bias. The black solid line is a simulation of the thermal radiation (*22*).

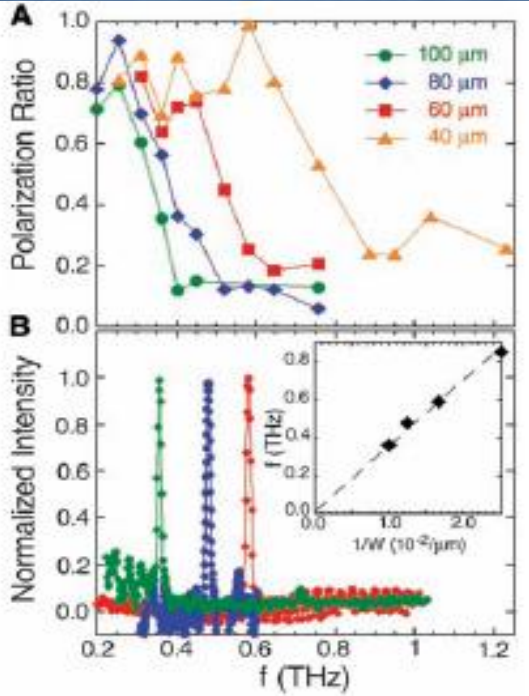

Fig. 3. Spectral characterization of the emission. **(A)** The polarization ratio—defined as the ratio the radiation power measured at perpendicular and at parallel filter settings—of the emission peaks is shown for four mesas as a function of cut-off frequency of the filters. The radiation frequency is estimated from the filter cut-off frequency at which the polarization ratio levels off at high frequencies (*22*). **(B)** Far-infrared spectra of the Josephson radiation. Sharp emission lines are clearly resolved. The observed line width of ~9 GHz (FWHM) is instrument-resolution limited. The scaling of the emission frequency with the inverse mesa width, shown in the inset, demonstrates that a cavity resonance on the width is excited.

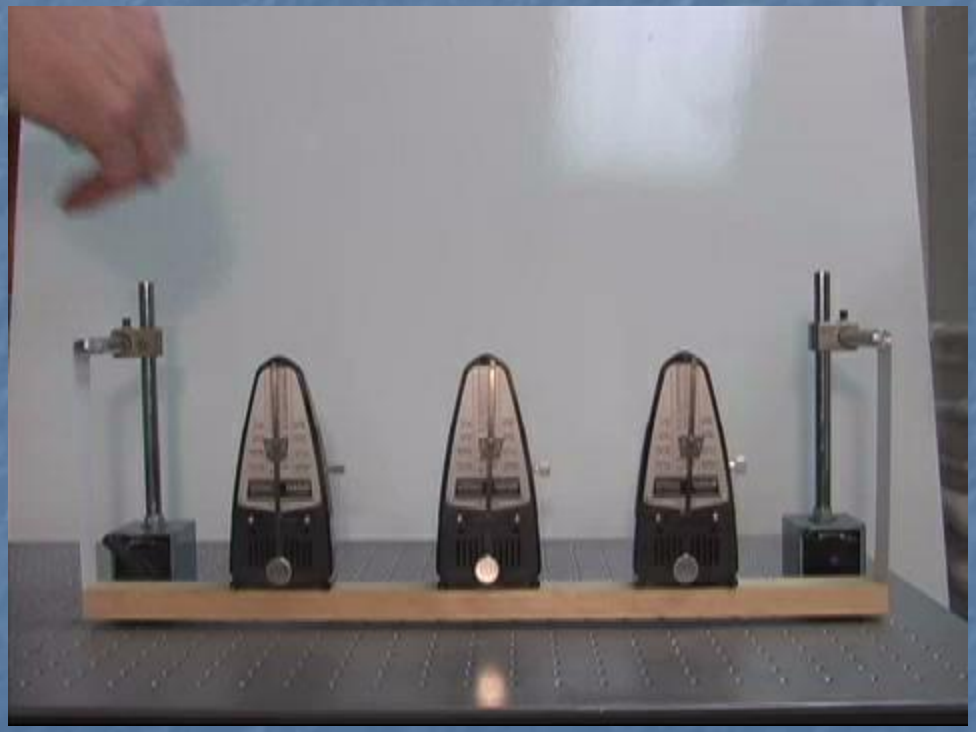

Models of JJ systems with capacitive coupling

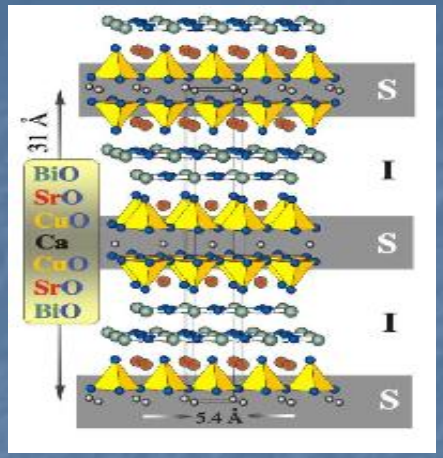

CCJJ

$$I = C\partial V/\partial t + \frac{V}{R} + I_c \sin\varphi$$

$$\frac{\hbar}{2e}\frac{\partial \varphi_{l,l+1}}{\partial t} = V_{l,l+1} + \frac{\varepsilon\mu^2}{d_s d_I}(V_{l+2,l+1} + V_{l-1,l} - 2V_{l,l+1})$$

CCJJ+DC

$$J_D^l = -\frac{\Phi_l - \Phi_{l+1}}{R}$$

$$J = C\frac{dV_l}{dt} + J_c^l \sin(\varphi_l) + \frac{\hbar}{2eR}\dot{\varphi}_l$$

$$\frac{\hbar}{2e}\frac{\partial \varphi_{l,l+1}}{\partial t} = V_{l,l+1} + \frac{\varepsilon\mu^2}{d_s d_I}(V_{l+2,l+1} + V_{l-1,l} - 2V_{l,l+1})$$

CIB

$$J_{qp}^l = \frac{\hbar}{2eR}\dot{\varphi}_l + \frac{\Psi_{l-1} - \Psi_l}{R}$$

$$\frac{\hbar}{2e}\dot{\varphi}_l(t) = (1+2a)V_l - a(V_{l-1} + V_{l+1}) + \Psi_l - \Psi_{l-1}$$

$$\rho_l = -\frac{\Phi_l}{4\pi\mu^2}; \qquad \Phi_l = \phi_l - \frac{\hbar}{2e}\frac{\partial\theta_l}{\partial t}; \qquad \alpha = \frac{\varepsilon\mu^2}{d_s d_I};$$

MODELS

* CCJJ-model:
  -T. Koyama and M. Tachiki, Phys. Rev. B 54, 16183 (1996)

* CCJJ+DC-model:
  -Yu. M. Shukrinov, F. Mahfouzi and P. Seidel, Physica C 449, 62 (2006).
  -M. Machida, T. Koyama, A. Tanaka and M. Tachiki, Physica C 331, 85 (2000).

* CIB-model:
  -D. A. Ryndyk, Phys. Rev. Lett. 80, 3376 (1998)

Модель ССДП с емкостной связью.

Схема системы СДП

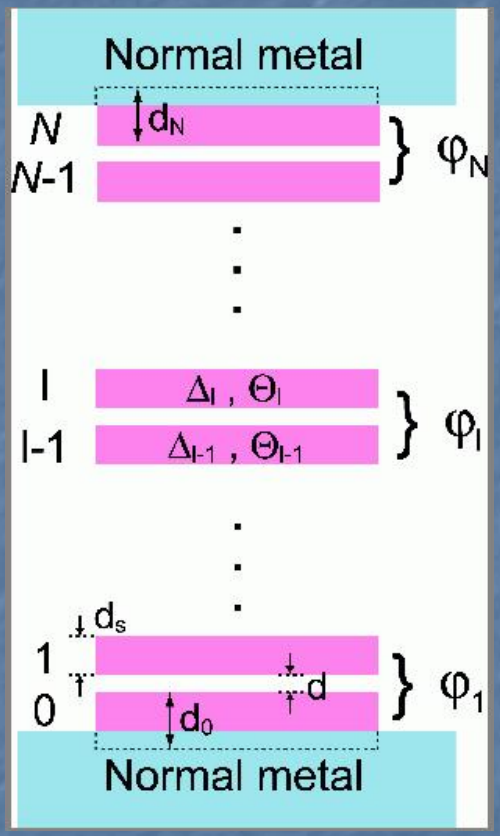

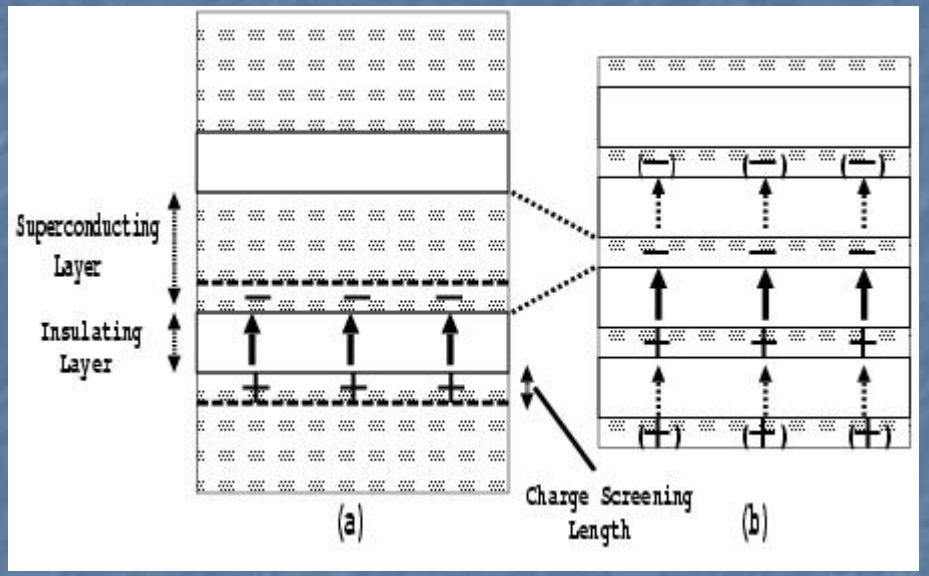

Generalized Josephson Relation

Gauge invariant phase difference:

$$\varphi_{l,l+1}(t) = \theta_l(t) - \theta_{l+1}(t) - \frac{2e}{\hbar}\int_l^{l+1} dz\, A_z(z,t)$$

$$\rho_l = -\frac{\Phi_l}{4\pi\mu^2}; \qquad \Phi_l = \phi_l - \frac{\hbar}{2e}\frac{\partial\theta_l}{\partial t}; \qquad \alpha = \frac{\varepsilon\mu^2}{d_s d_I};$$

Generalized Josephson Relation :

$$\frac{\partial\varphi_{l,l+1}}{\partial t} = \frac{2e}{\hbar}V_{l,l+1} + \frac{2e}{\hbar}(\Phi_{l+1} - \Phi_l); \qquad V_{l,l+1} = \int_l^{l+1} dz E_z(z,t)$$

$$GJR: \quad \frac{\partial\varphi_{l,l+1}}{\partial t} = \frac{2e}{\hbar}V_{l,l+1} + \frac{2e}{\hbar}4\pi\mu^2(\rho_{l+1} - \rho_l)$$

$$div\,\varepsilon E = 4\pi\rho; \qquad E = \frac{V}{d_I} \qquad \rho_l = \frac{\varepsilon}{4\pi d_s d_I}(V_{l,l+1} - V_{l-1,l})$$

$$GJR: \qquad \frac{\hbar}{2e}\frac{\partial\varphi_{l,l+1}}{\partial t} = V_{l,l+1} + \frac{\varepsilon\mu^2}{d_s d_I}(V_{l+2,l+1} + V_{l-1,l} - 2V_{l,l+1})$$

CCJJ model (Koyama, Tachiki, 1996)

$$I = C\partial V/\partial t + \frac{V}{R} + I_c \sin\varphi$$

$$\frac{\hbar}{2e}\dot{\varphi}_l = \sum_{l'=1}^{n} A_{ll'} V_{l'}$$

$$\partial^2 \varphi_l/\partial t^2 = \sum_{l'} A_{ll'}[I - \sin\varphi_{l'}] - \beta\partial\varphi_l/\partial t$$

$$\alpha = \frac{\mu^2 \varepsilon}{d_s d_I}$$

$$A = \begin{pmatrix} 1+\alpha G & -\alpha & 0 & \dots & & & \\ -\alpha & 1+2\alpha & -\alpha & 0 & \dots & & \\ 0 & -\alpha & 1+2\alpha & -\alpha & 0 & \dots & \\ \dots & \dots & \dots & \dots & \dots & \dots & \dots \\ & & & \dots & 0 & -\alpha & 1+\alpha G \end{pmatrix}$$

$$\tau = \omega_p t$$

$$\omega_p^2 = \frac{2eI_c}{\hbar C}$$

$$A = \begin{pmatrix} 1+2\alpha & -\alpha & 0 & \dots & & & -\alpha \\ -\alpha & 1+2\alpha & -\alpha & 0 & \dots & & \\ 0 & -\alpha & 1+2\alpha & -\alpha & 0 & \dots & \\ \dots & \dots & \dots & \dots & \dots & \dots & \dots \\ -\alpha & & & \dots & 0 & -\alpha & 1+2\alpha \end{pmatrix}$$

$$V_c = I_c R_N = \frac{\hbar\omega_c}{2e}$$

$$\beta = \frac{1}{\omega_p RC}$$

$$\beta^2 = \frac{1}{\beta_c}, \qquad \beta_c = \omega^2 R^2 C^2 = \frac{\omega_c^2}{\omega_p^2} = CR_N\omega_c$$

$$G = 1 + \gamma, \quad \gamma = d_s / d_{1,N}$$

Numerical Procedure

$$\frac{d^2}{dt^2}\varphi_l = (I - \sin\varphi_l - \beta\frac{d\varphi_l}{dt}) + \alpha(\sin\varphi_{l+1} + \sin\varphi_{l-1} - 2\sin\varphi_l)$$

$$\bar{V}_l = \frac{1}{T_{\max} - T_{\min}} \int_{T_{\min}}^{T_{\max}} V_l dt \qquad V = \sum_{l=1}^{N} \bar{V}_l$$

$$R - state: \quad < \frac{\partial\varphi}{\partial t} >= const, < \sin\varphi >= 0$$

$$O - state: \quad < \frac{\partial\varphi}{\partial t} >= 0, < \sin\varphi >= const$$

Time dependence

- div ($\varepsilon\varepsilon_0$ E) = Q

$Q_l = Q_0\ \alpha\ (V_{l+1} - V_l)$

$Q_0 = \varepsilon\ \varepsilon_0\ V_0 / r_D^2$

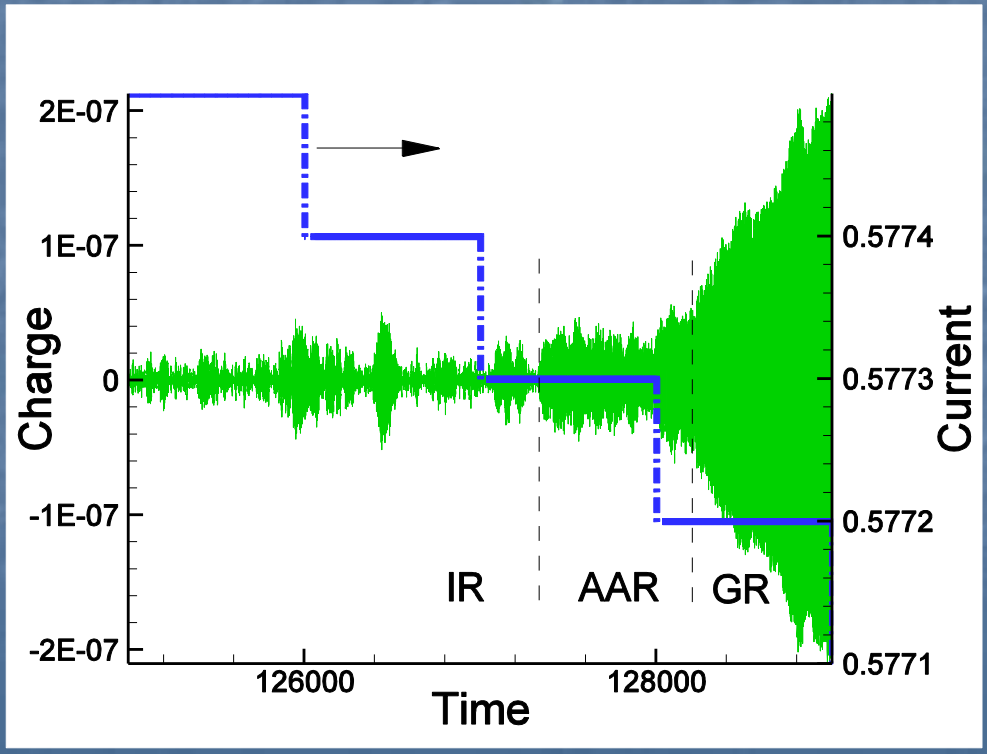

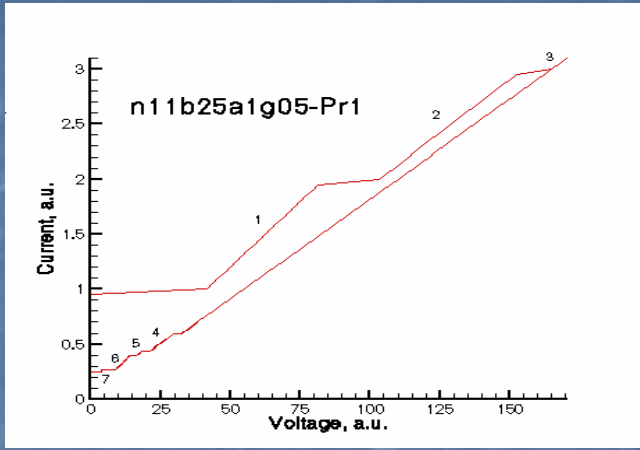

$$S => R_1[1,4,6,8,11] => R_2[5^-,7^-] => R_3 => R_4[3^-,6^-,9^-] =>$$
$$=> R_5[1,2,4,8,10,11] => R_6[1,4,8,11] => R_7[1,11] => S$$

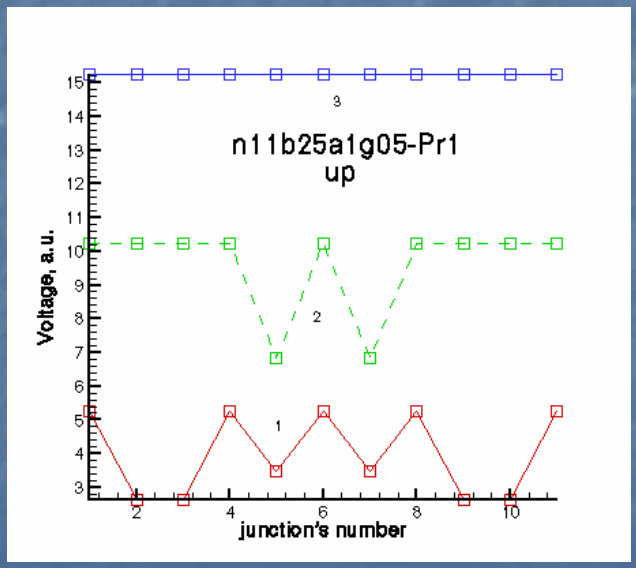

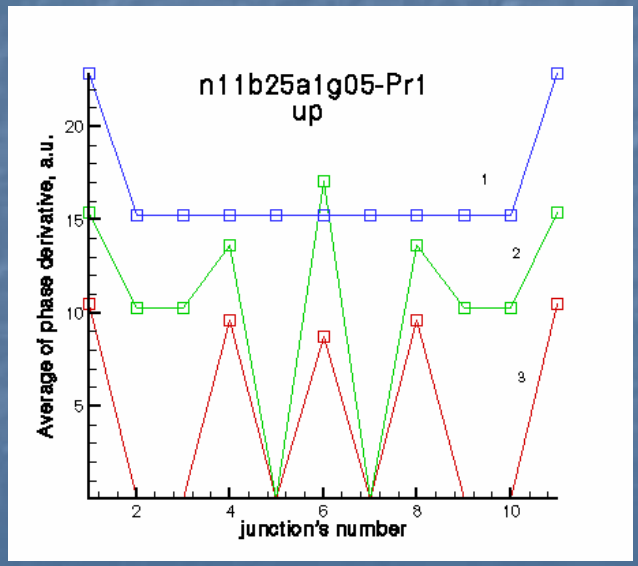

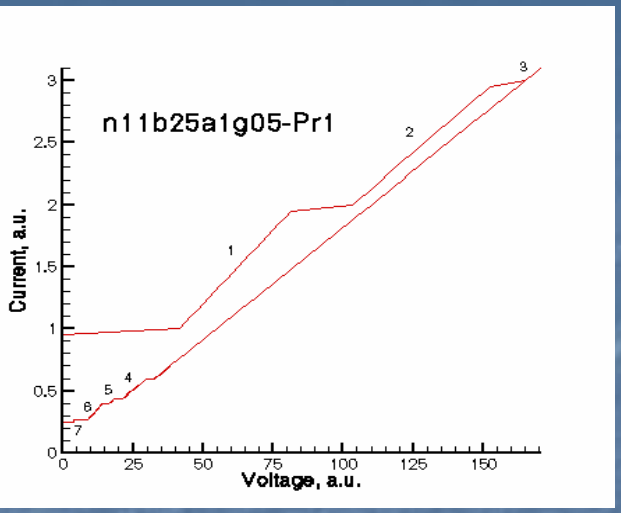

$$S => R_1[1,4,6,8,11] => R_2[5^-,7^-] => R_3 => R_4[3^-,6^-,9^-] =>$$
$$=> R_5[1,2,4,8,10,11] => R_6[1,4,8,11] => R_7[1,11] => S$$

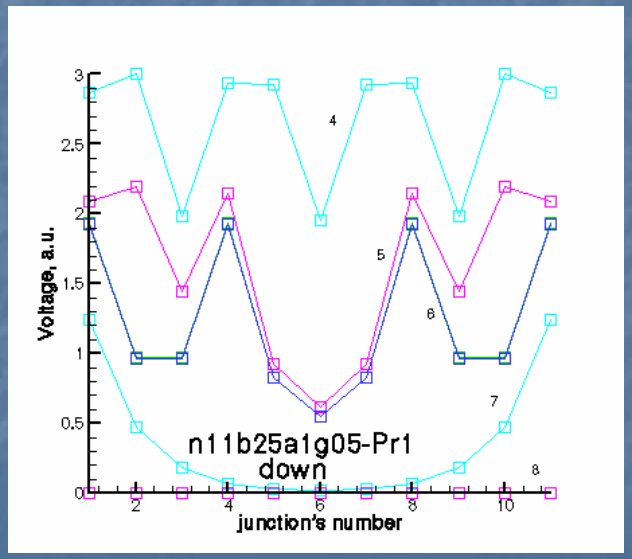

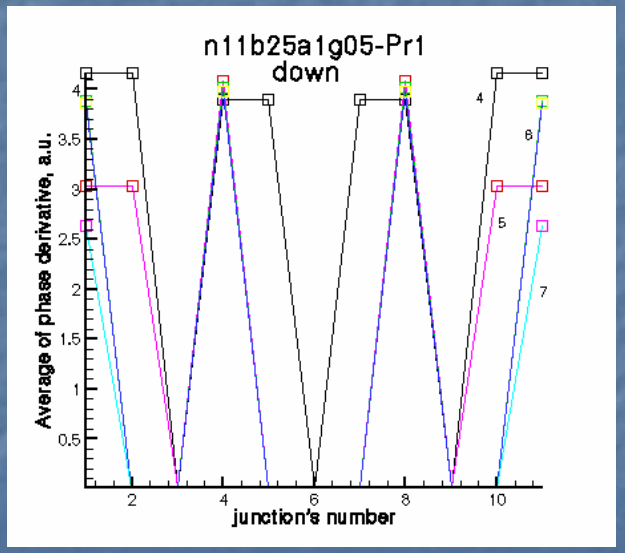

Result of calculation

$$\frac{d^2\varphi_{l,l+1}}{d\tau^2} = (1 - \alpha\nabla^{(2)})(J/J_c - \sin(\varphi_{l,l+1})) - \beta\frac{d\varphi_{l,l+1}}{d\tau}$$

$$\frac{\hbar}{2e}\dot{\varphi}_{l,l+1} = (1 - \alpha\nabla^{(2)})V_{l,l+1}$$

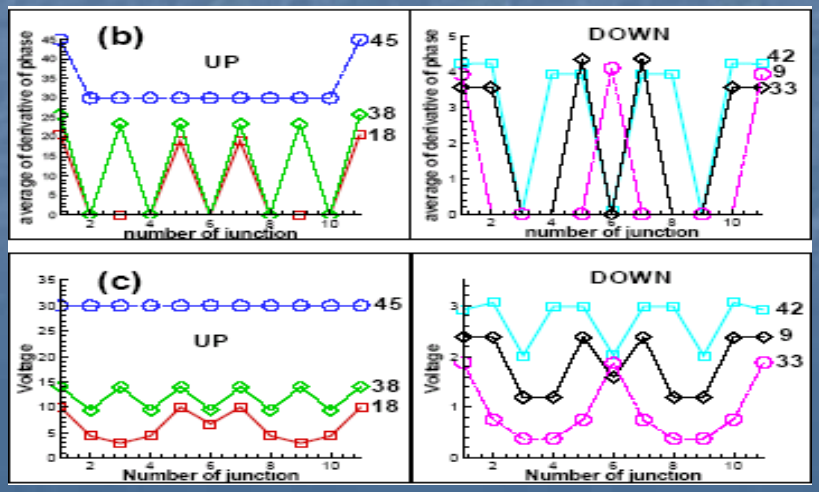

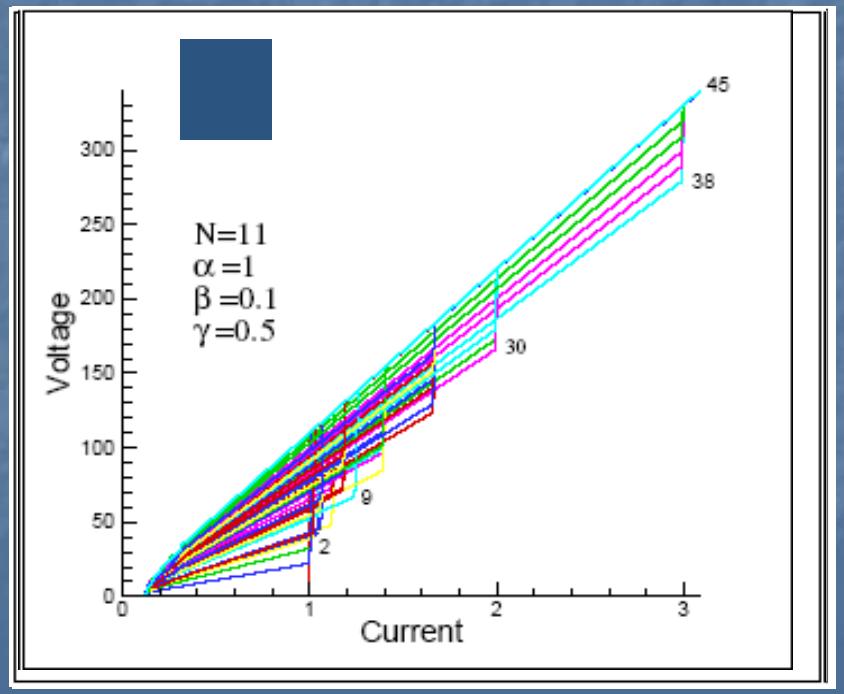

TABLE I: Branch's number, slopes and corresponding states for IVC of 11 IJJ in CCJJ model at $\alpha = 1, \beta = 0.1$ and $\gamma = 0.5$.

branch	*state*	*slope*	*branch*	*state*	*slope*
0 :	S	0	29 :	$R(3,4,5,6,7,8,9)$	80.77
1 :	$R(6)$	22.27	30 :	$R(1,3,6,9,11)$	83.33
2 :	$R(1,11)$	32.36	30 :	$R(1,4,6,8,11)$	83.33
3 :	$R(5,7)$	38.80	31 :	$R(2,4,6,8,10)$	84.67
4 :	$R(2,10)$	40.34	32 :	$O(3,5,6,7,9)$	84.76
5 :	$R(5,6,7)$	42.13	32 :	$O(2,5,6,7,10)$	84.76
6 :	$R(3,9)$	42.99	33 :	$O(3,4,6,8,9)$	86.67
7 :	$R(4,8)$	43.19	33 :	$O(2,3,6,9,10)$	86.67
8 :	$R(1,2,10,11)$	52.34	34 :	$O(1,4,6,8,11)$	88.00
9 :	$R(1,6,11)$	54.00	34 :	$O(1,3,6,9,11)$	88.00
10 :	$R(4,6,8)$	55.10	35 :	$O(4,5,7,8)$	90.00
11 :	$R(4,5,7,8)$	58.43	35 :	$O(3,4,8,9)$	90.00
12 :	$R(2,3,9,10)$	60.22	35 :	$O(2,3,9,10)$	90.00
13 :	$R(3,6,9)$	60.77	36 :	$O(1,5,7,11)$	91.33
14 :	$R(2,6,10)$	60.86	36 :	$O(1,4,8,11)$	91.33
15 :	$R(4,5,6,7,8)$	61.76	36 :	$O(1,5,7,11)$	91.33
16 :	$R(3,4,8,9)$	62.20	37 :	$O(5,6,7)$	91.43
17 :	$R(1,3,9,11)$	65.56	38 :	$O(2,4,8,10)$	93.33
18 :	$R(1,5,7,11)$	69.523	39 :	$O(1,6,11)$	94.67
19 :	$R(3,5,7,9)$	70.77	40 :	$O(3,5,7,9)$	96.67
20 :	$R(1,4,8,11)$	71.43	40 :	$O(2,5,7,10)$	96.67
21 :	$R(1,2,3,9,10,11)$	72.22	40 :	$O(3,5,7,9)$	96.67
22 :	$R(2,4,8,10)$	72.76	41 :	$O(1,11)$	98.000
23 :	$R(1,2,6,10,11)$	72.86	42 :	$O(4,6,8)$	100.00
23 :	$R(1,5,6,7,11)$	72.86	42 :	$O(3,6,9)$	100.00
24 :	$R(3,4,6,8,9)$	74.10	42 :	$O(4,6,8)$	100.00
24 :	$R(3,5,6,7,9)$	74.10	43 :	$O(5,7)$	103.33
25 :	$R(2,5,7,10)$	74.67	43 :	$O(4,8)$	103.33
26 :	$R(3,4,5,7,8,9)$	77.44	43 :	$O(3,9)$	103.33
27 :	$R(2,3,6,9,10)$	78.00	43 :	$O(5,7)$	103.33
27 :	$R(2,5,6,7,10)$	78.00	44 :	$O(6)$	106.67
28 :	$R(2,3,4,8,9,10)$	79.43	45 :	R	110.00

M.Machida, T.Koyama

PHYSICAL REVIEW B 70, 024523 (2004)

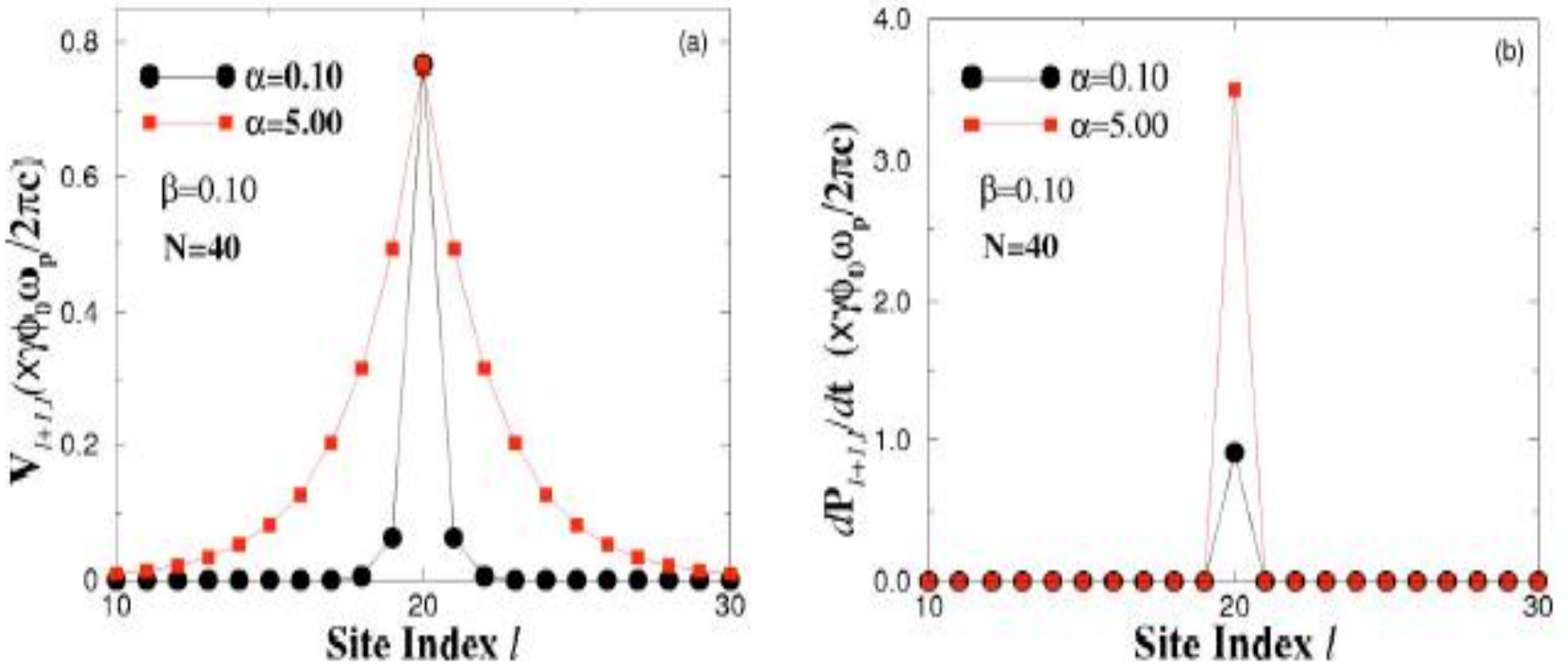

FIG. 3. (Color online) (a) Voltage distribution (Ref. 21) in the first branch for α=0.10 and α=5.00. The periodic boundary condition is imposed on the system with N=40; (b) distribution of $dP_{\ell+1,\ell}/(dt)$.

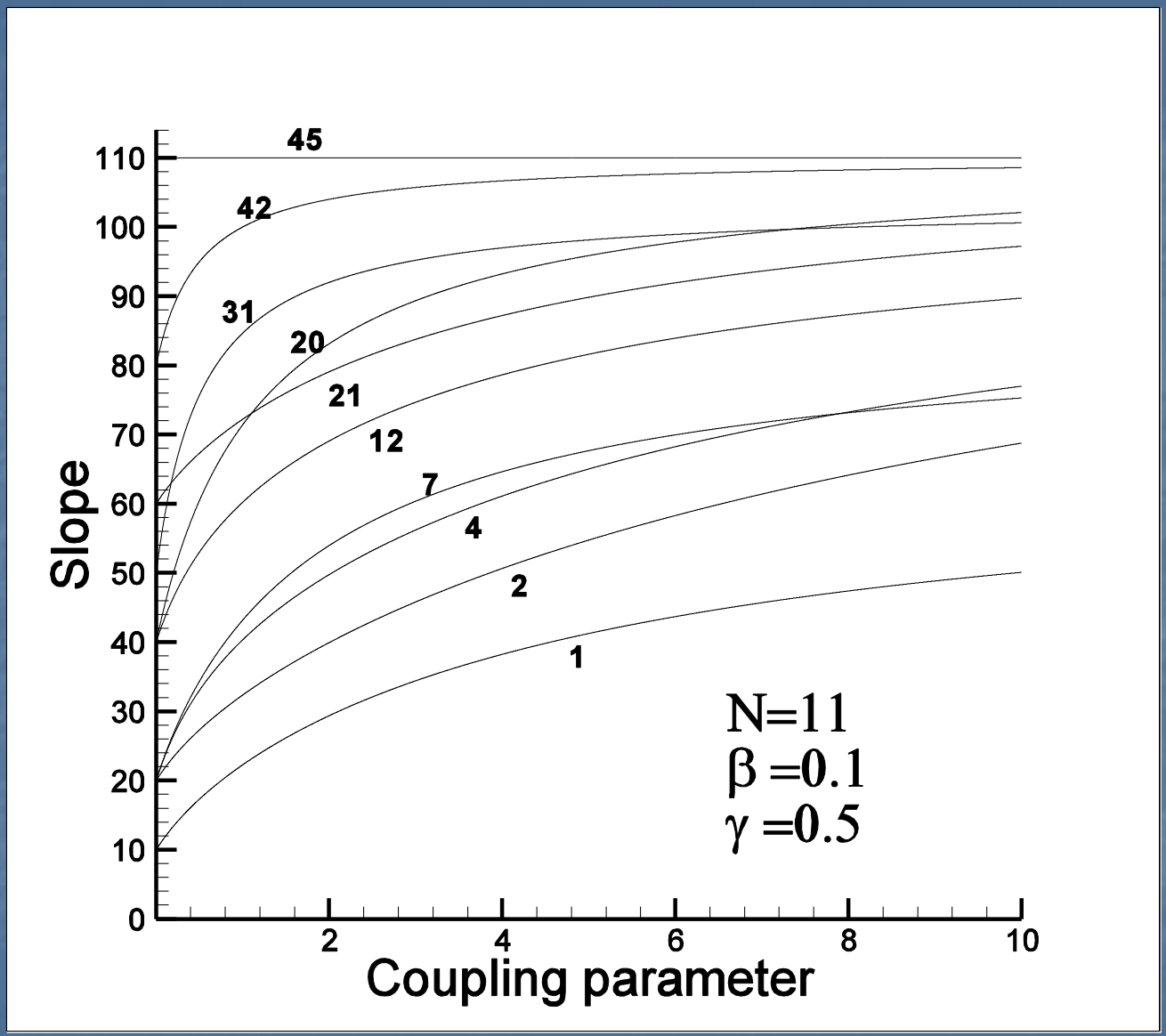
45
42
31
20
21
12
7
4
2
1
N=11
β =0.1
γ =0.5
Slope
Coupling parameter
0
10
20
30
40
50
60
70
80
90
100
110
2
4
6
8
10

CVC in CCJJ model

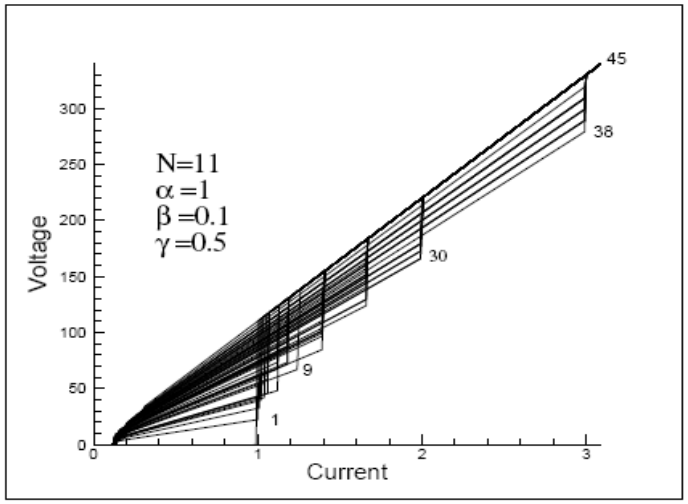

FIG. 1: The total branch structure in the IVC of IJJ. The branch's numbers correspond to the states shown in Table of Ref.[13].

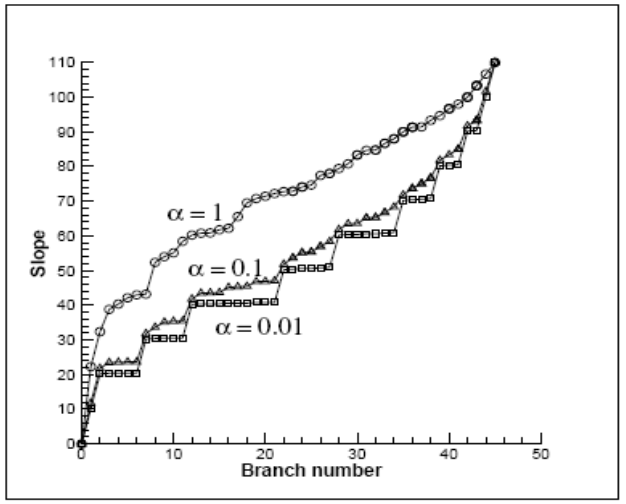

FIG. 2: The dependence of the slope versus branch number at different values of coupling parameter.

Shukrinov, F. Mahfouzi, Physica C 434 (2006) 6-12.

CCJJ+DC model

$$J = C\partial V/\partial t + V/R + J_C \sin\varphi$$

$$J_D^l = -\frac{\Phi_l - \Phi_{l+1}}{R}$$

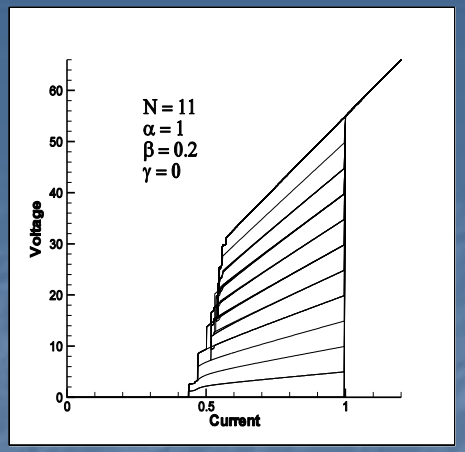

$$J = C\frac{dV_l}{dt} + J_c^l \sin(\varphi_l) + \frac{\hbar}{2eR}\dot{\varphi}_l$$

$$\ddot{\varphi}_l = \sum_{l'=1}^{n} A_{ll'}\left[\frac{J}{J_c} - \sin(\varphi_{l'}) - \beta\dot{\varphi}_{l'}\right]$$

$$A = \begin{pmatrix} 1+\alpha G & -\alpha & 0 & \dots & & \\ -\alpha & 1+2\alpha & -\alpha & 0 & \dots & \\ 0 & -\alpha & 1+2\alpha & -\alpha & 0 & \dots \\ \dots & \dots & \dots & \dots & \dots & \dots \\ & & & \dots & 0 & -\alpha & 1+\alpha G \end{pmatrix}$$

$$A = \begin{pmatrix} 1+2\alpha & -\alpha & 0 & \dots & & -\alpha \\ -\alpha & 1+2\alpha & -\alpha & 0 & \dots & \\ 0 & -\alpha & 1+2\alpha & -\alpha & 0 & \dots \\ \dots & \dots & \dots & \dots & \dots & \dots \\ -\alpha & & & \dots & 0 & -\alpha & 1+2\alpha \end{pmatrix}$$

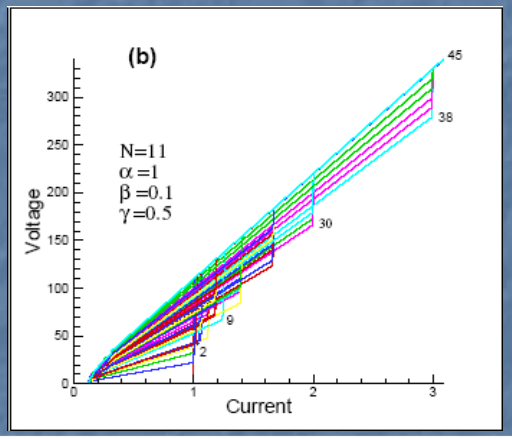

$$\frac{d^2}{dt^2}\varphi_l = (I - \sin\varphi_l - \beta\frac{d\varphi_l}{dt})$$
$$+\alpha(\sin\varphi_{l+1} + \sin\varphi_{l-1} - 2\sin\varphi_l)$$
$$+\alpha\beta(\frac{d\varphi_{l+1}}{dt} + \frac{d\varphi_{l-1}}{dt} - 2\frac{d\varphi_l}{dt})$$

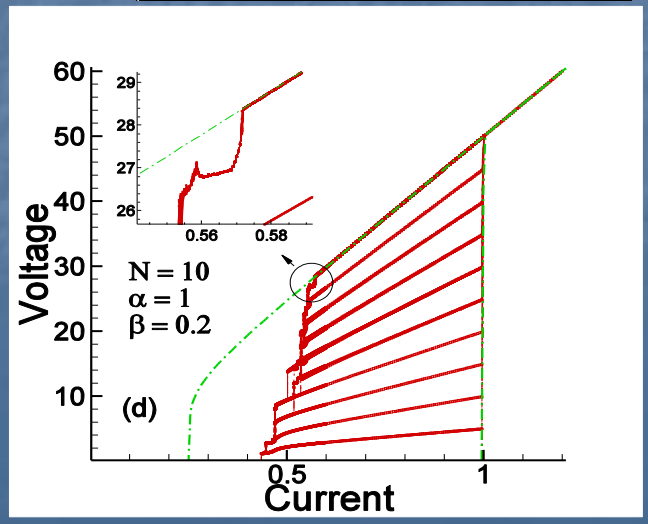

Yu. M. Shukrinov, F. Mahfouzi and P. Seidel, Physica C 449, 62-66 (2006)

The branch structure in IVC in CCJJ+DC model at different beta

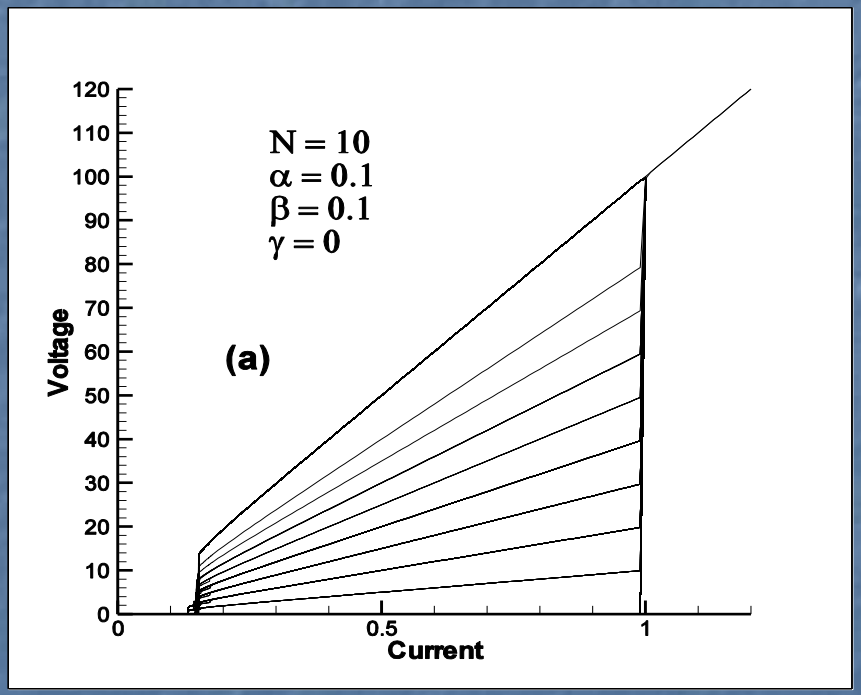

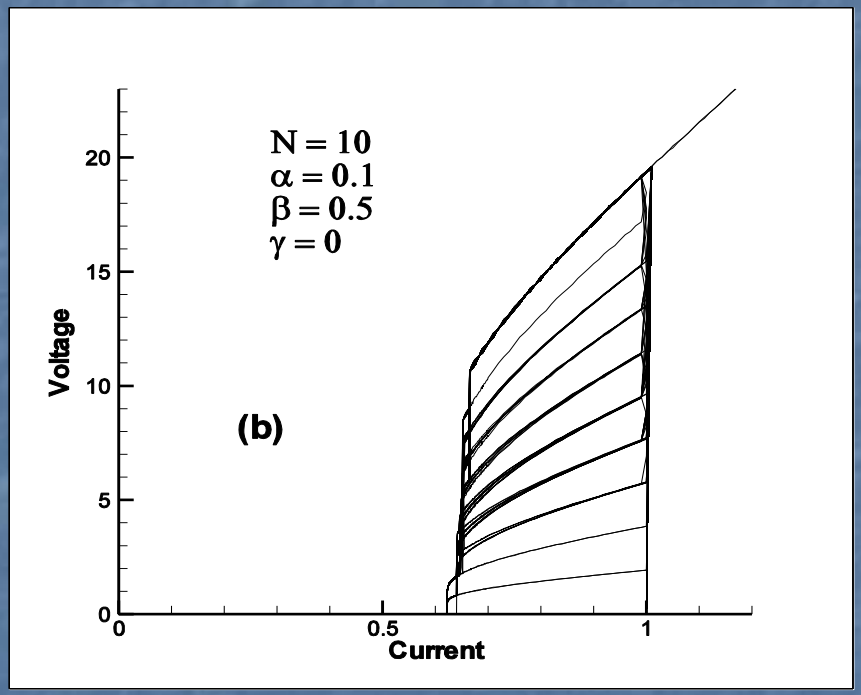

The branch structure in IVC in CCJJ+DC model at different boundary conditions

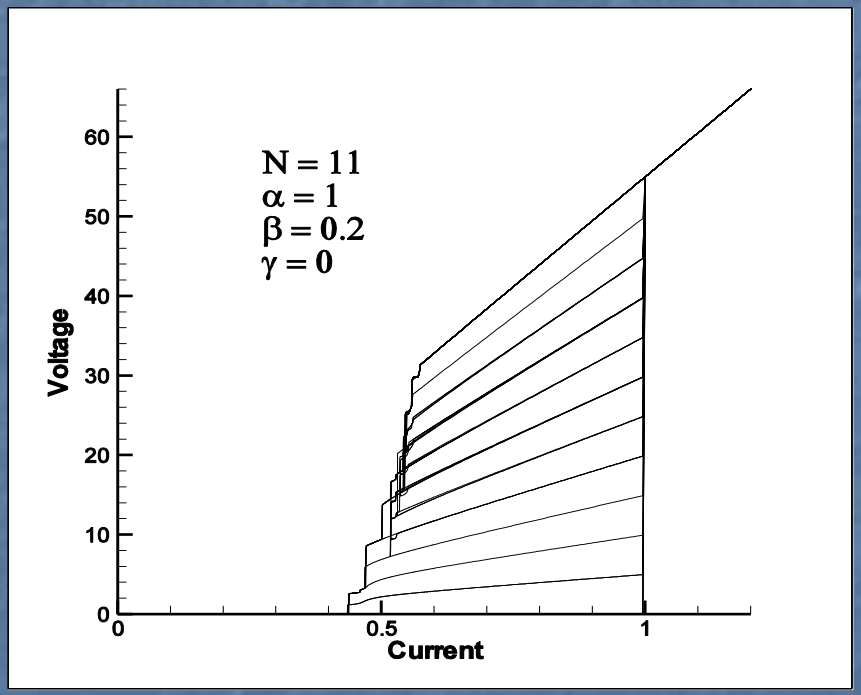

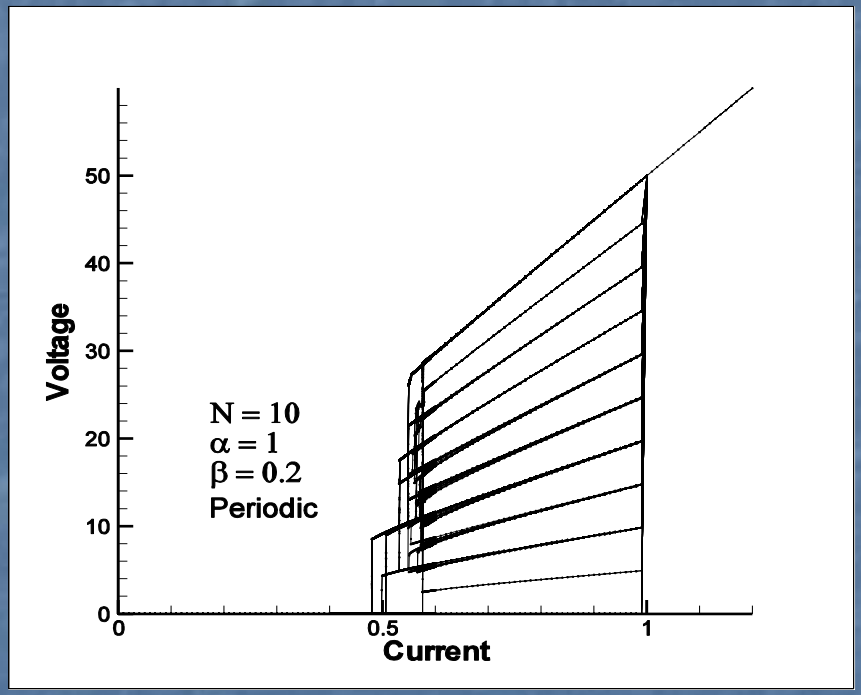

Параметрический резонанс в ССДП

Equation for difference of phase differences

By subtracting equation (1) for $(l)th$ and $(l-1)th$ junctions we have

$$(\ddot{\varphi}_l - \ddot{\varphi}_{l-1}) + (1 - \alpha\nabla^{(2)})\{\sin(\varphi_l) - \sin(\varphi_{l-1}) + \beta(\dot{\varphi}_l - \dot{\varphi}_{l-1})\} = 0$$

In linear approximation for difference of phase differences, $\delta_l = \varphi_l - \varphi_{l-1}$, we obtain

$$\ddot{\delta}_l + (1 - \alpha\nabla^{(2)})(\cos(\varphi)\delta_l + \beta\dot{\delta}_l) = 0$$

Expanding $\delta_l(t)$ in the Fourier series

$$\delta_l(t) = \sum_k \delta_k e^{ikl}$$

and taking into account, that

$$\nabla^{(2)} e^{ikl} = 2(\cos(k) - 1)e^{ikl}$$

we get

$$\ddot{\delta}_k + (1 + 2\alpha(1 - \cos(k)))(\beta\dot{\delta}_k + \cos(\varphi)\delta_k) = 0.$$

Equation for difference of phase differences

We consider that in rotating state $\varphi \simeq \Omega t = \frac{1}{N} V t$.
Introducing new dimensionless parameters,

$$\tau = \omega_p(k) t$$

$$\omega_p(k) = \omega_p \sqrt{1 + 2\alpha(1 - \cos(k))}$$

$$\beta(k) = \beta \sqrt{1 + 2\alpha(1 - \cos(k))}$$

$$\Omega(k) = \Omega \frac{1}{\sqrt{1 + 2\alpha(1 - \cos(k))}}$$

equation (9) can be written as

$$\ddot{\delta_k} + \beta(k)\dot{\delta_k} + \cos(\Omega(k)\tau)\delta_k = 0.$$

Parametric resonance region

$$\ddot{\delta}_k + \beta(k)\dot{\delta}_k + \cos(\Omega(k)\tau)\delta_k = 0$$

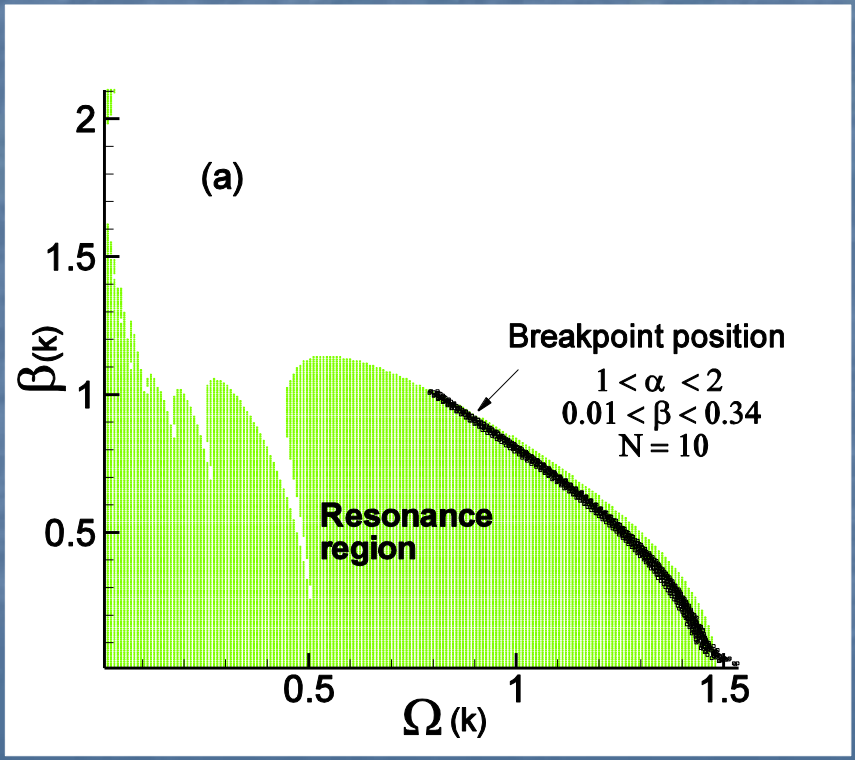

$$\varphi = \Omega t = \frac{1}{N} V t$$

$$\tau = \omega_p(k) t$$

$$\omega_p(k) = \omega_p \sqrt{1 + 2\alpha(1 - \cos k)}$$

$$\beta(k) = \beta \sqrt{1 + 2\alpha(1 - \cos k)}$$

$$\Omega(k) = \frac{\Omega}{\sqrt{1 + 2\alpha(1 - \cos k)}}$$

Charge oscillations near the breakpoint in the stack with 9 JJ

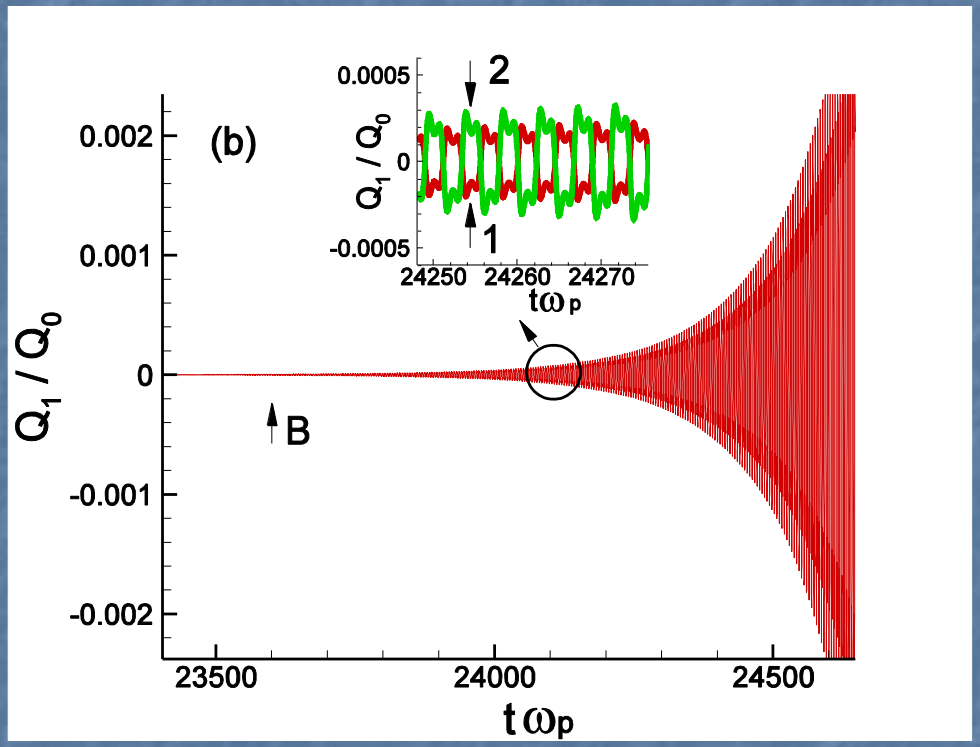

Test of the exponential dependence of charge amplitude.

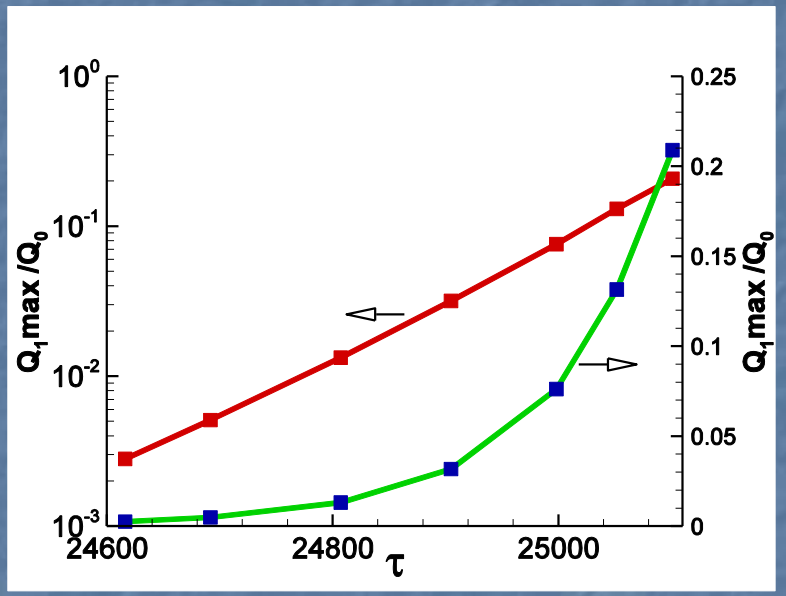

Yu.M.Shukrinov, F.Mahfouzi, M.Suzuki
Phys.Rev.B 78, 134521 (2008).

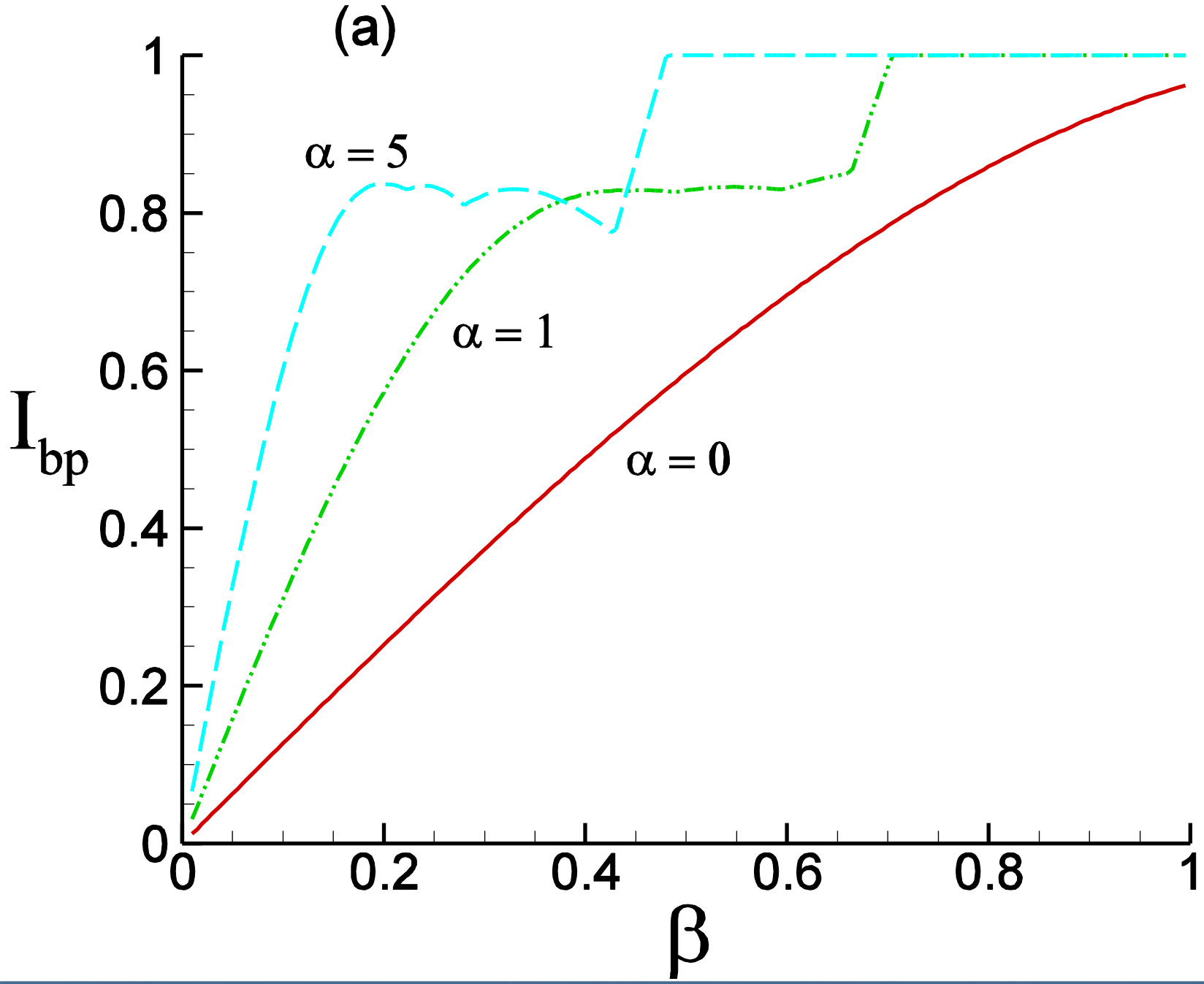
(a)
α = 5
α = 1
α = 0
I_bp
β
0
0.2
0.4
0.6
0.8
1

The ♋♌♂dependence of the BPC of the outermost branch of IVC for stack of 10 IJJ at PBC.

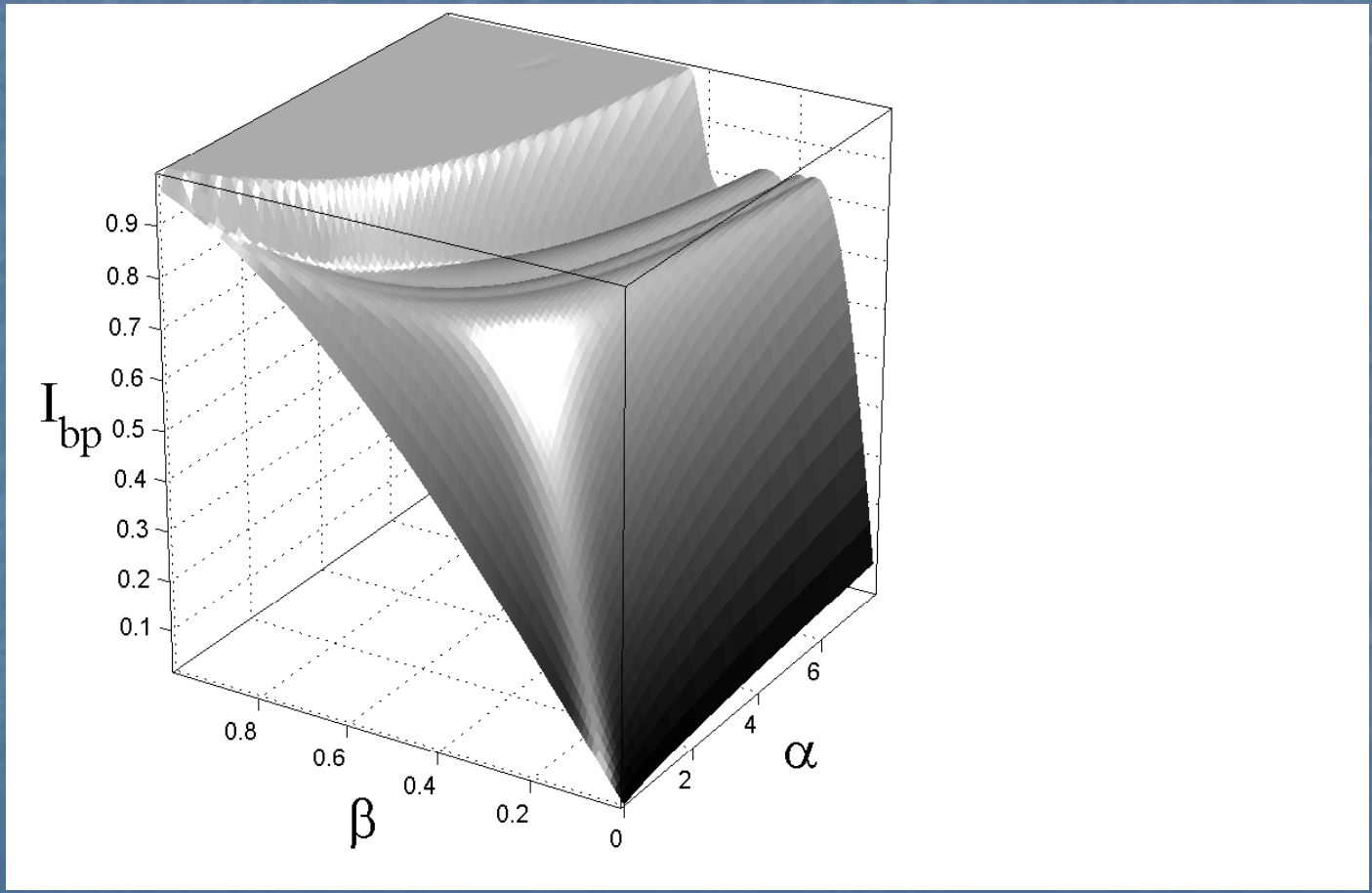

Yu.M.Shukrinov, F.Mahfouzi. Phys.Rev.Lett, 98, 157001 (2007)

(a,b) - The ♋ – and ♌ dependence of the BPC at PBC.
(c) - Charge distribution among the junctions in the stack for different plasma modes.

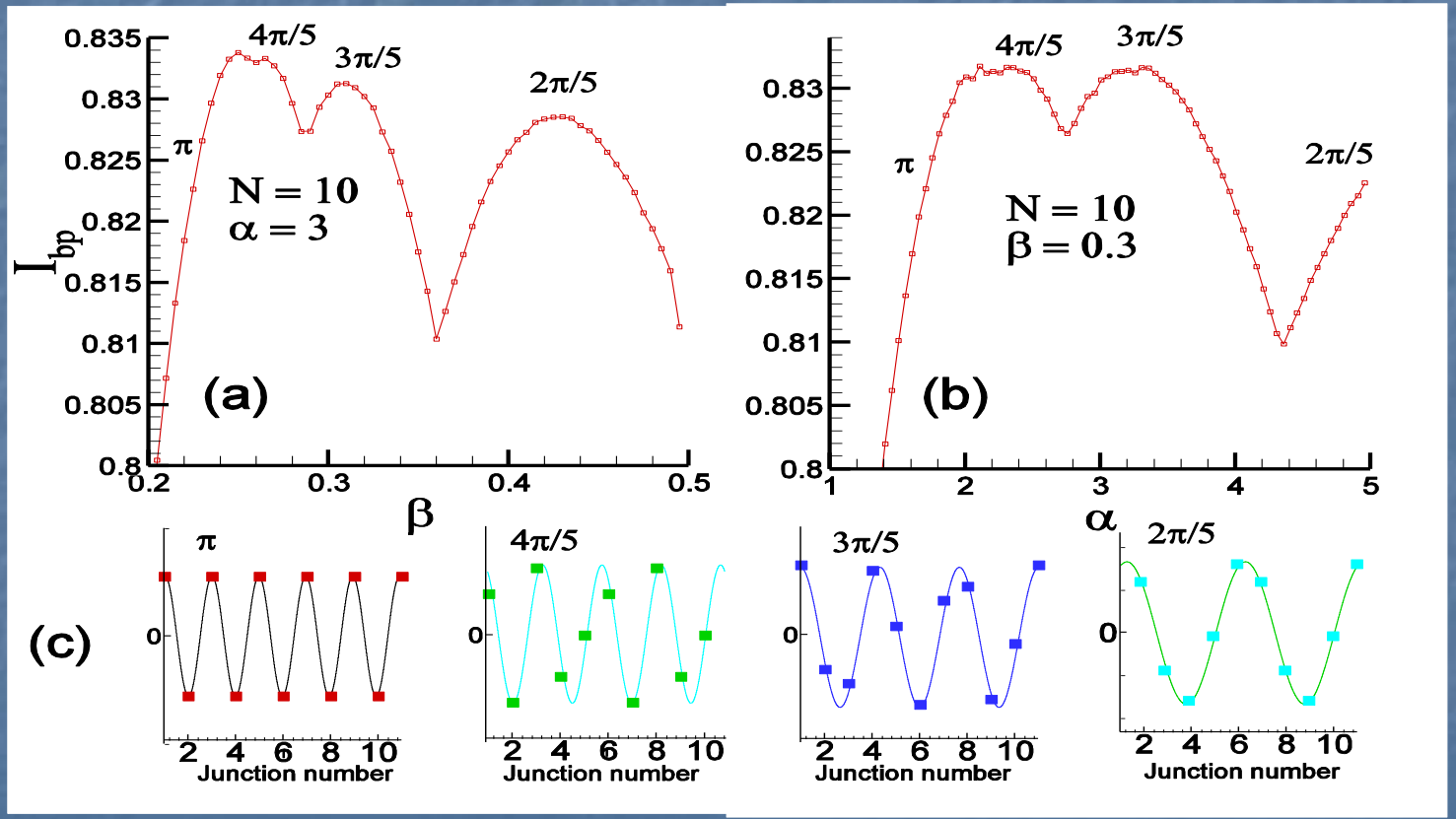

$\beta = 0.24$

$\beta = 0.27$

$\beta = 0.3$

$\beta = 0.4$

Yu.M.Shukrinov, F.Mahfouzi. Phys.Rev.Lett, 98, 157001 (2007)

IVC of the outermost branch for the stacks with different number N of IJJ at ♑ and at PBC

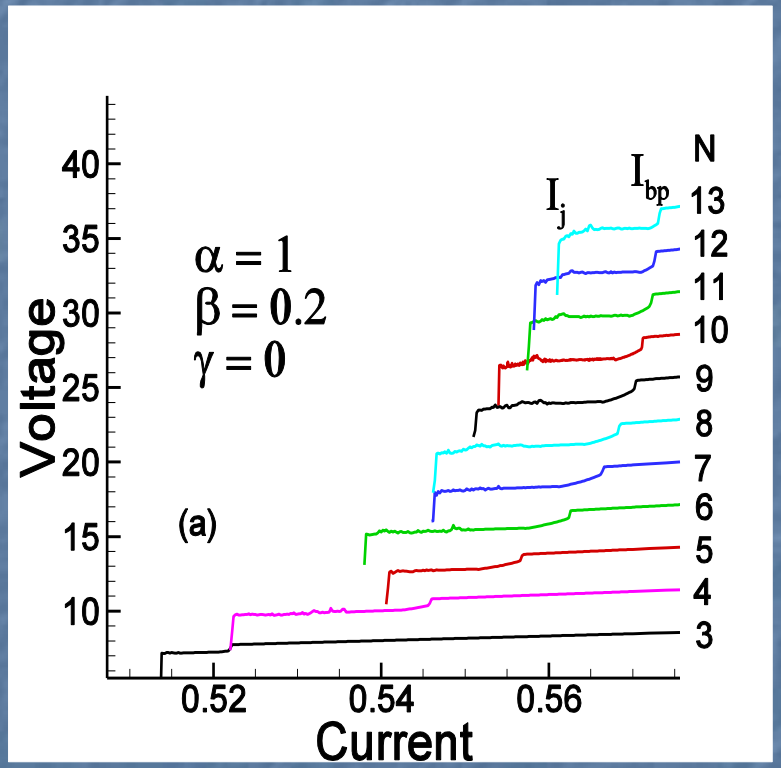

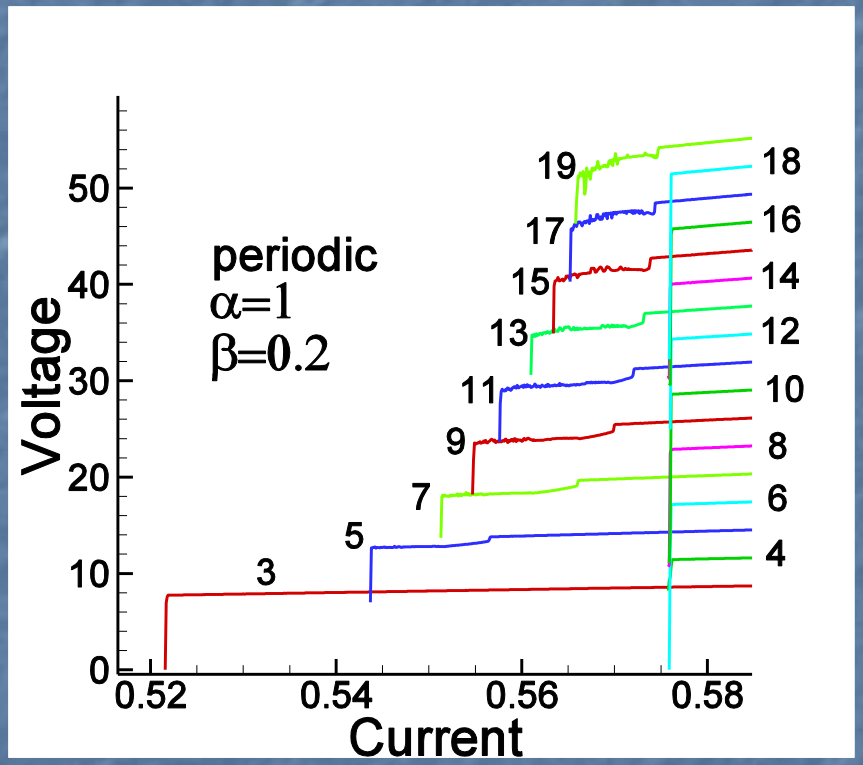

$k = \pi \qquad k = (N-1)\pi / N$

Yu.M.Shukrinov, F.Mahfouzi, N.F.Pedersen. Phys.Rev.B 75, 104508 (2007).

(a)-Parametric resonance region; (b) - Modeling of the BPC for plasma modes with k = □ and k = 2□/5 for stack of 10 IJJ at PBC; (c), (d)- Modeling of the BPC from resonance region.

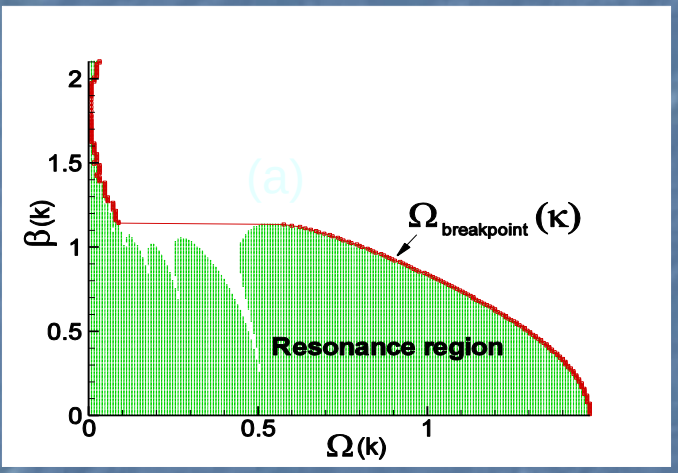

$$I_{bp} = \beta\sqrt{1 + 2\alpha(1 - \cos k)}\,\Omega_{bp}(k, \beta)$$

$$V_{bp} / N = I_{bp} / \beta$$

$$\Omega_{bp} = V_{bp} / \left[N\sqrt{1 + 2\alpha(1 - \cos k)} \right]$$

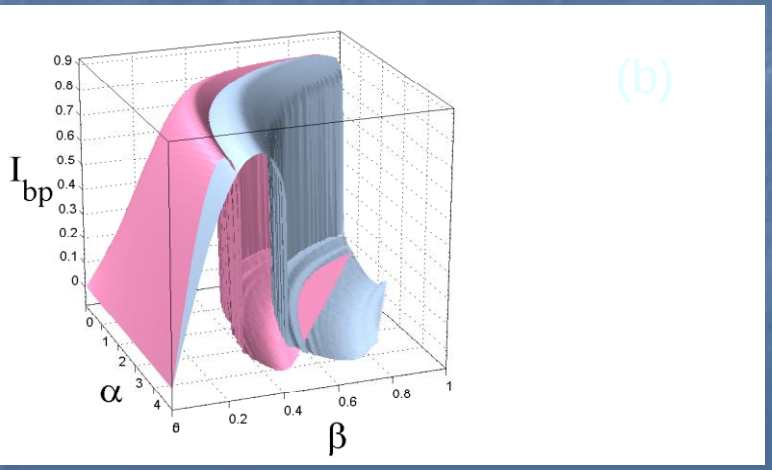

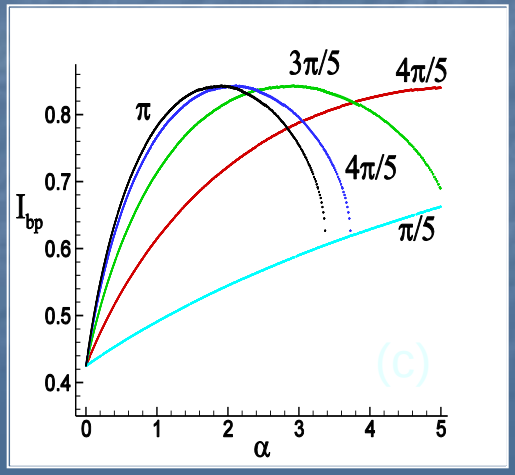

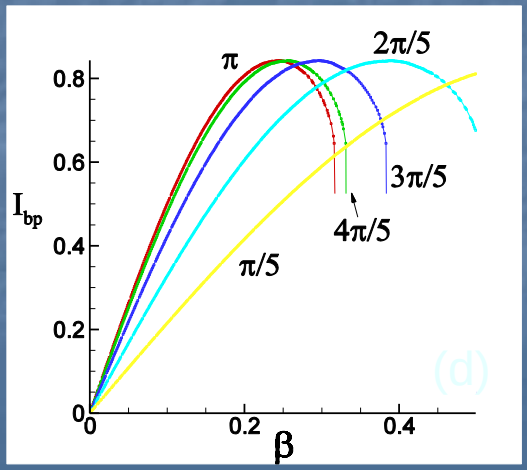

Yu.M.Shukrinov, F.Mahfouzi. Phys.Rev.Lett, 98, 157001 (2007)

Сравнение результатов расчета и моделирования

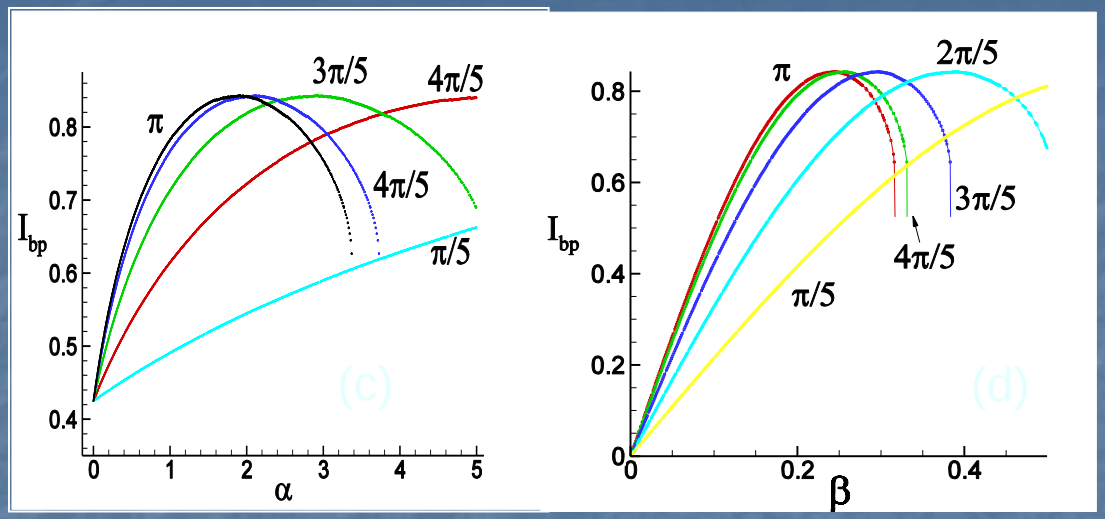

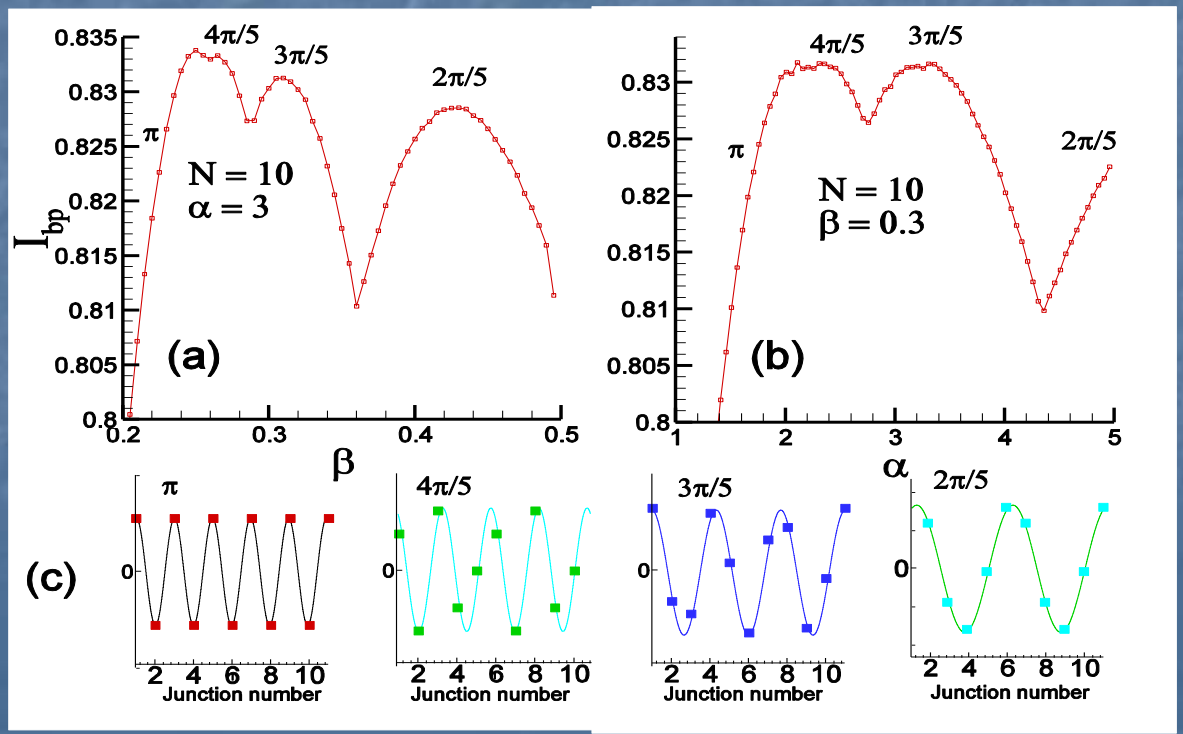

Modeled and calculated dependence of the BPC

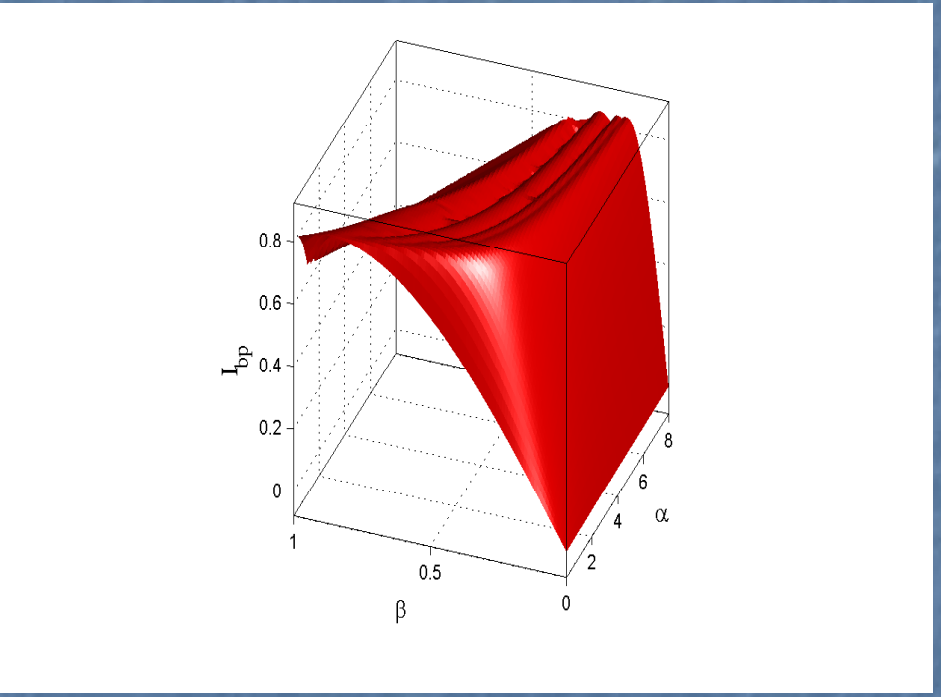

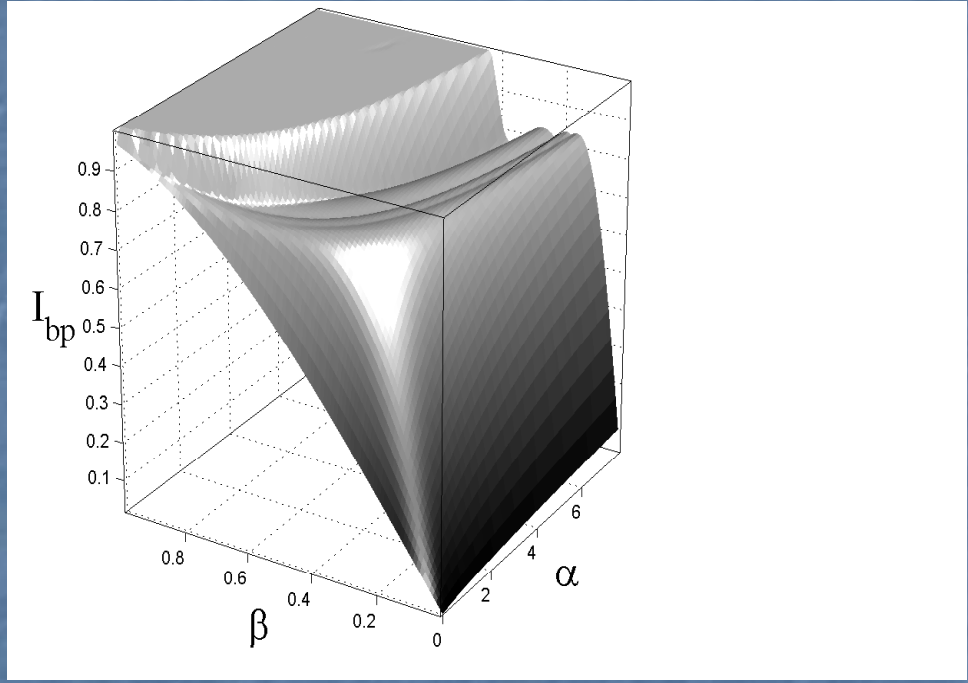

The simulated IVC of the outermost branch in the stack with different number of junctions

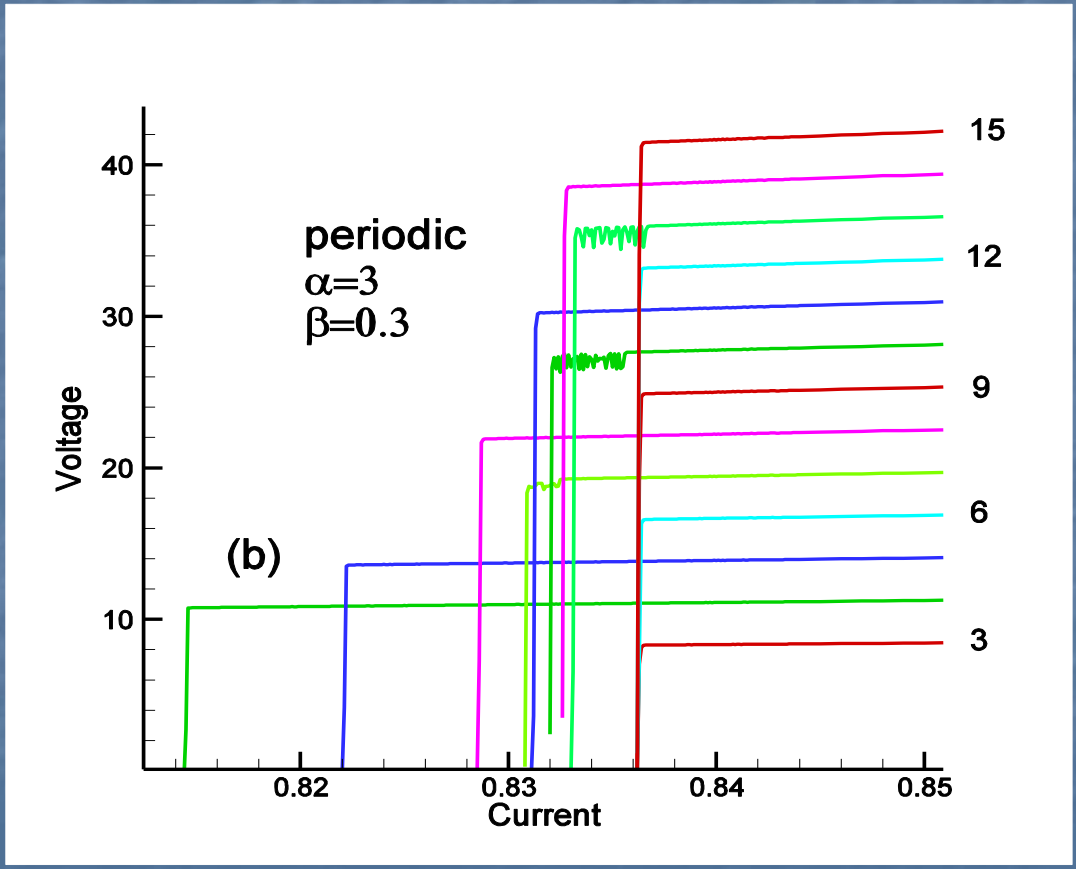

The β_L-dependence of the BPC for the stacks with different number of IJJ.

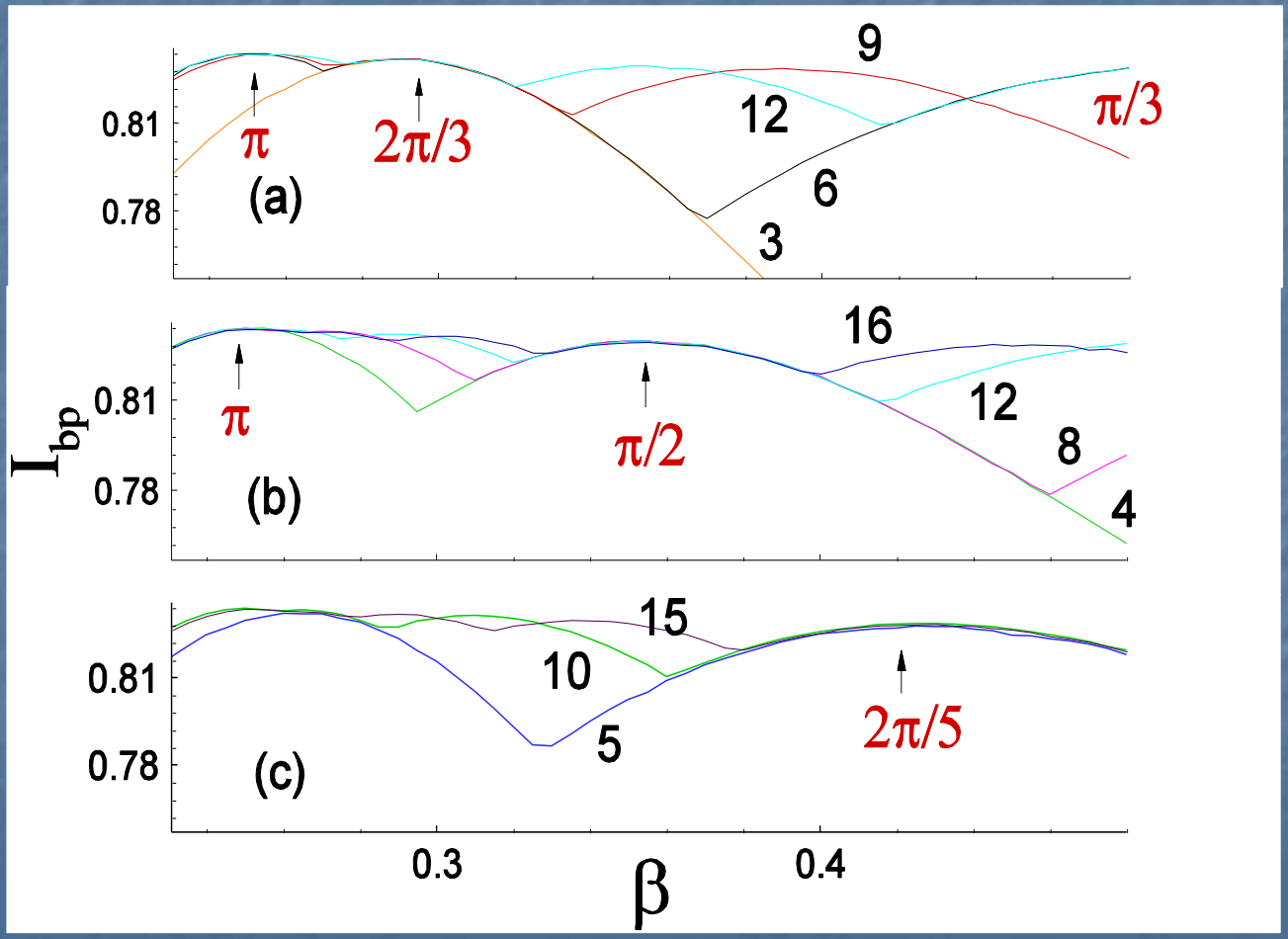

The simulated IVC of the outermost branch in the stacks with different number of junctions

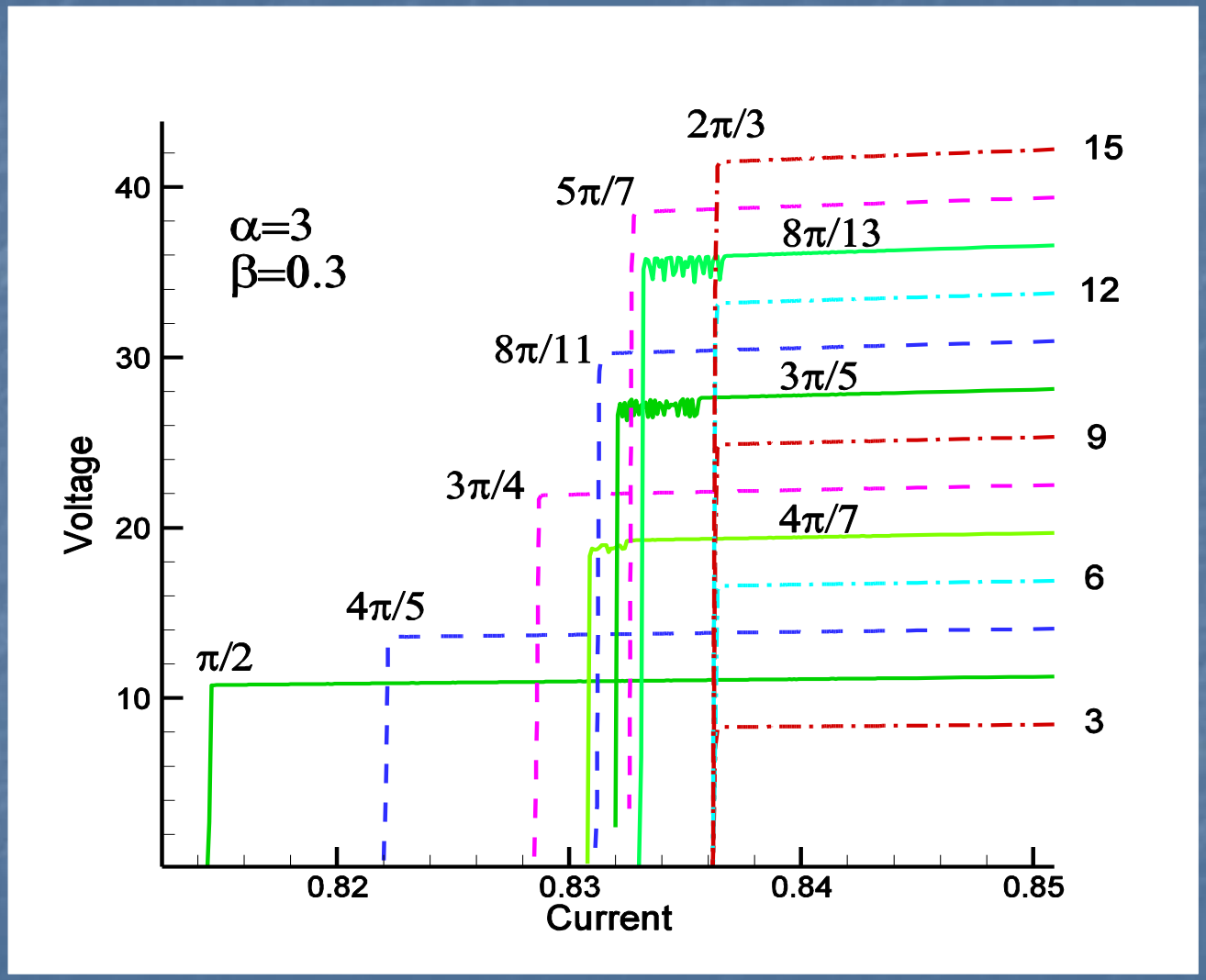

$N = 3n, \quad k = \frac{2\pi}{3}$ $\qquad N = 3n+1, \quad k = \frac{2(N-1)\pi}{3N}$ $\qquad N = 3n+2, \quad k = \frac{2(N+1)\pi}{3N}$

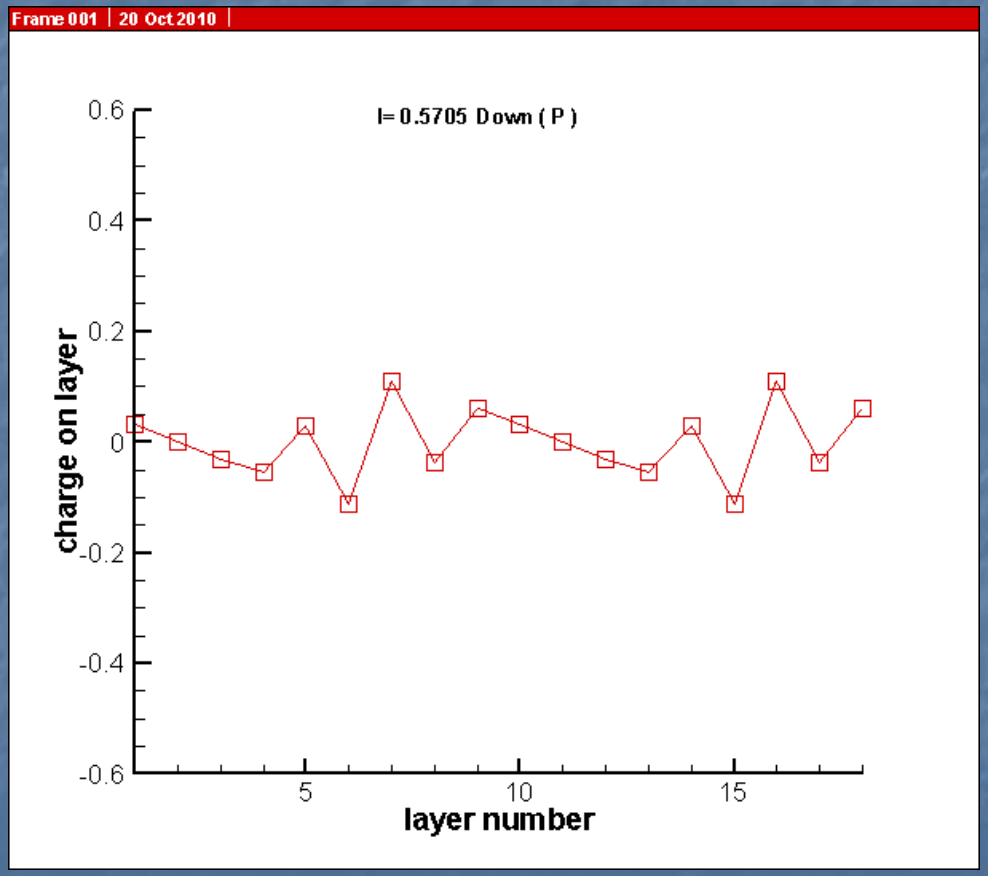
Frame 001 | 20 Oct 2010
I= 0.5705 Down (P)
0.6
0.4
0.2
0
-0.2
-0.4
-0.6
charge on layer
5
10
15
layer number

Модель с разбалансом ветвей в спектре элементарных возбуждений сверхпроводника (CIB модель)

Collective Dynamics of Intrinsic Josephson Junctions in High-T_c Superconductors

Dmitry A. Ryndyk*

The key point of our theory is a nonequilibrium nature of the ac Josephson effect in layered superconductors [18,20–22]. It means that superconducting layers are in the nonstationary nonequilibrium state due to the injection of quasiparticles and Cooper pairs, and a nonzero invariant potential

$$\Phi_i(t) = \phi_i - (\hbar/2e)(\partial\theta_i/\partial t)$$

is generated inside them, where ϕ_i is the electrostatic potential and θ_i is the phase of superconducting condensate,

$$\rho_i = -2e^2 N(0)(\Phi_i - \Psi_i) = -\frac{1}{4\pi r_D^2}(\Phi_i - \Psi_i), \tag{2}$$

where Ψ_i is determined by the electron-hole charge imbalance

$$e\Psi_i = -\int_\Delta^\infty (n_\epsilon^i - n_{-\epsilon}^i)\, d\epsilon, \tag{3}$$

where we use the averaged-over-momentum-direction quasiparticle distribution function n_ϵ^i introduced by Eliashberg [26], which describes quasielectron (at $\epsilon > 0$) and quasihole (at $\epsilon < 0$) energy distributions, $|\epsilon|$ is the quasiparticle energy. In equilibrium $n_\epsilon^i = n_{-\epsilon}^i = n_\epsilon^{(0)} = 1/2[1 - th(|\epsilon|/2T)]$.

CIB-model

$$\ddot{\varphi}_l = \sum_{m=1}^{N} A_{lm}[\frac{J}{J_c} + I_{rand} - J_c(1-\kappa\psi_{m-1}^2)(1-\kappa\psi_m^2)\sin(\varphi_m) -$$

$$\beta\dot{\varphi}_m + \psi_m - \psi_{m-1}] + \frac{\dot{\psi}_l - \dot{\psi}_{l-1}}{\beta}$$

$$\zeta\dot{\psi}_0 = \eta\gamma_d(\frac{J}{J_c} - \beta\dot{\varphi}_1 + \psi_1 - \psi_0) - \gamma_\tau\psi_0$$

$$\zeta\dot{\psi}_l = \eta(\beta(\dot{\varphi}_{l-1} - \dot{\varphi}_l) + \psi_{l-1} + \psi_{l+1} - 2\psi_l) - \psi_l$$

$$\zeta\dot{\psi}_N = \eta\gamma_d(\beta\dot{\varphi}_N - \frac{J}{J_c} + \psi_{N-1} - \psi_N) - \gamma_\tau\psi_N$$

$$V_l = (1-\alpha\nabla^{(2)})^{-1}(\dot{\varphi}_l + \frac{\psi_l - \psi_{l+1}}{\beta})$$

$$\psi_l = \Psi_l/J_cR,\ \omega_p = \sqrt{\frac{2eJ_c}{\hbar C}},\ \beta = \frac{\hbar\omega_p}{2eRJ_c}, \zeta = \omega_p\tau_{qp}, \eta = \frac{4\pi r_D^2\tau_{qp}}{d_s R}, \gamma_d = \frac{d_s}{d_s^0} = \frac{d_s}{d_s^n}, \gamma_\tau = \frac{\tau_{qp}}{\tau_{qp}^0} = \frac{\tau_{qp}}{\tau_{qp}^n}$$

Resonance regions in CIB-model

$$\ddot{\delta_k} + \cos(\varphi)\delta_k + (\beta(k) - \frac{\eta(k)}{\zeta})\dot{\delta_k}$$

$$+(1 + \frac{\eta(k)+1}{\zeta\beta(k)})\eta(k)\beta(k)\int_0^\tau dt\dot{\delta_k}e^{\frac{1+\eta(k)}{\zeta\beta(k)}(t-\tau)} + \triangle\psi_0 e^{-\frac{1+\eta(k)}{\zeta\beta(k)}\tau} = 0,$$

ψ' и $\eta(k)$ определены как $\psi' = 2(1 - \cos(k))\psi$ и $\eta(k) = 2(1 - \cos(k))\eta$.

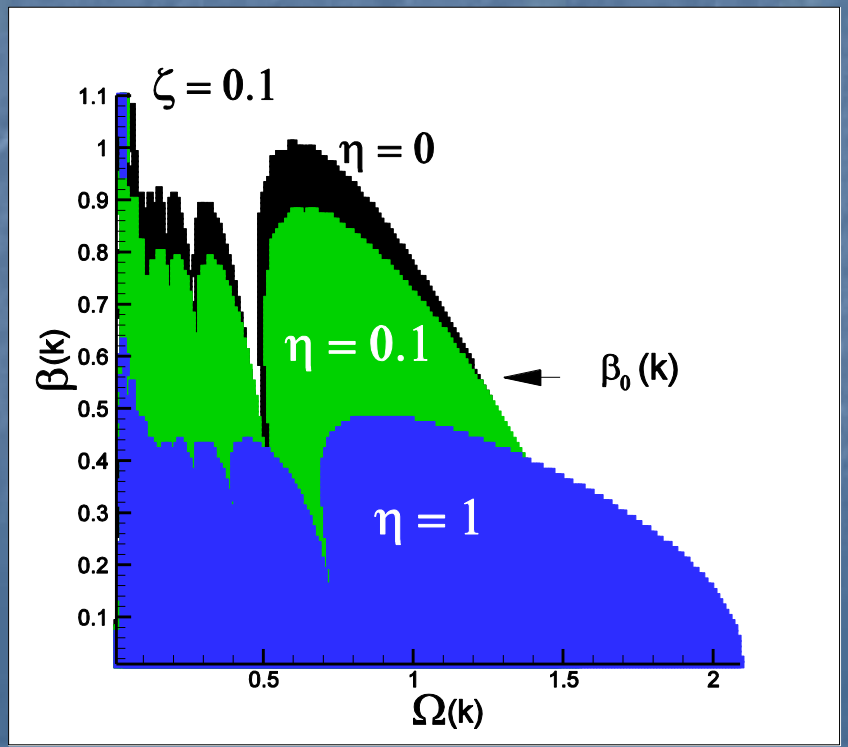

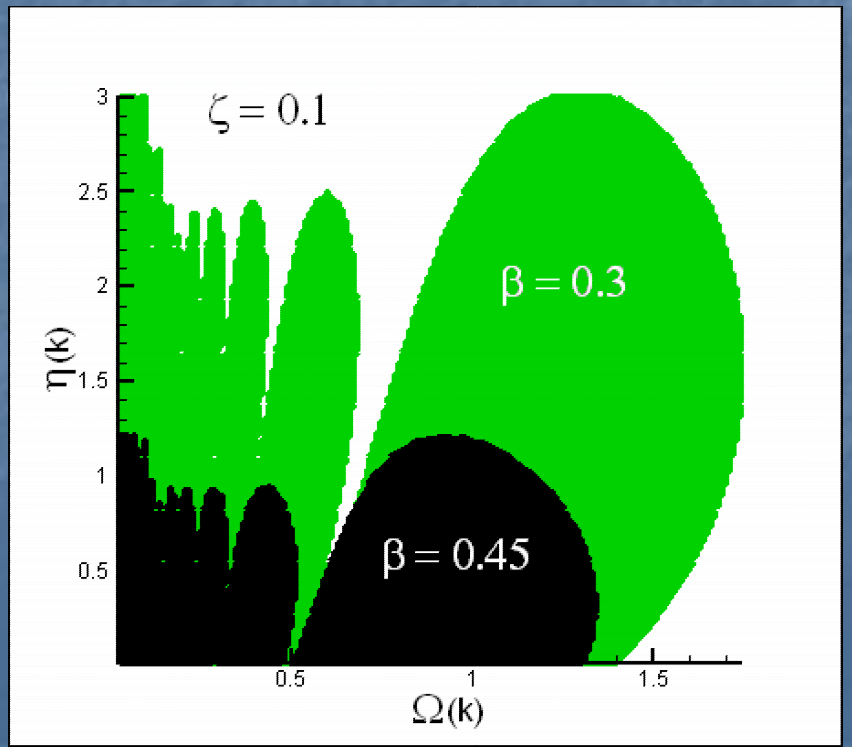

CVC at different coupling

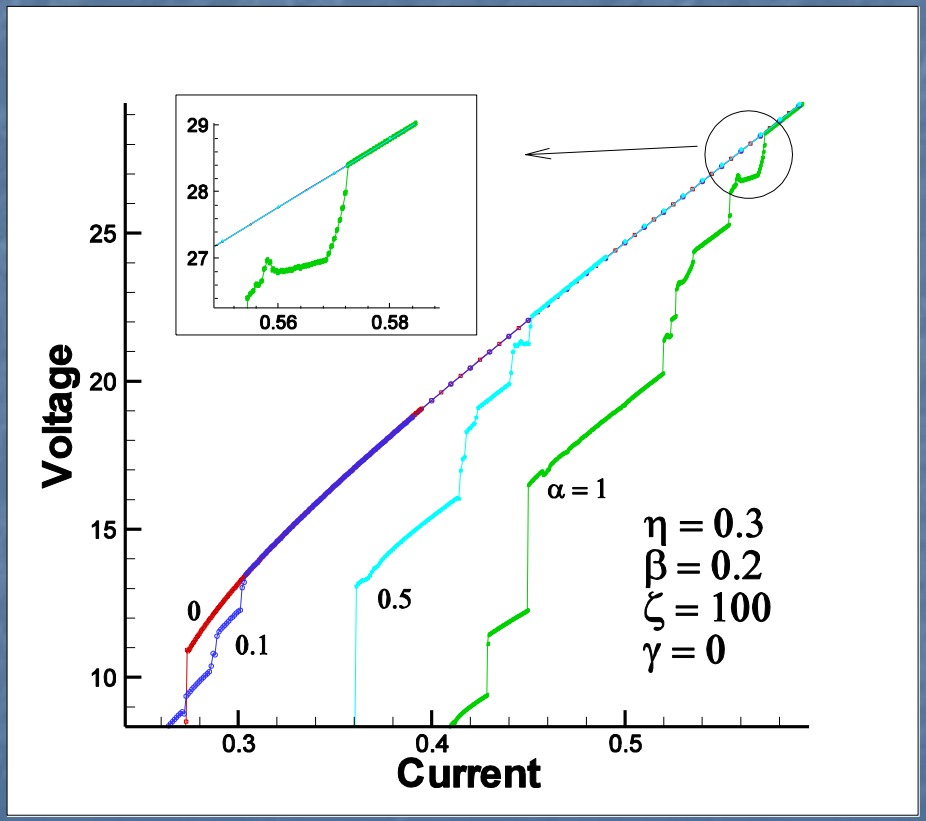

CVC in CIB-model

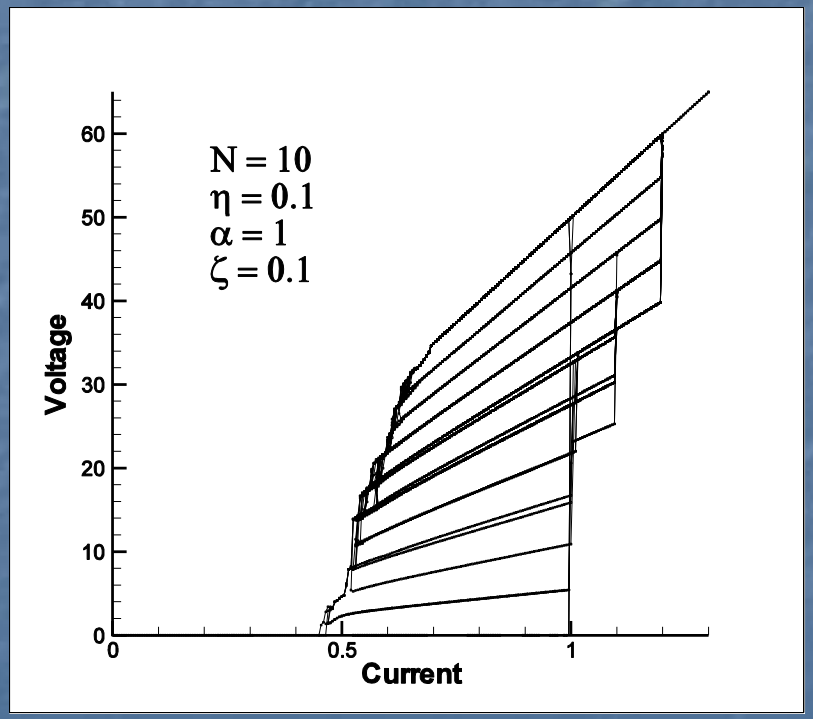

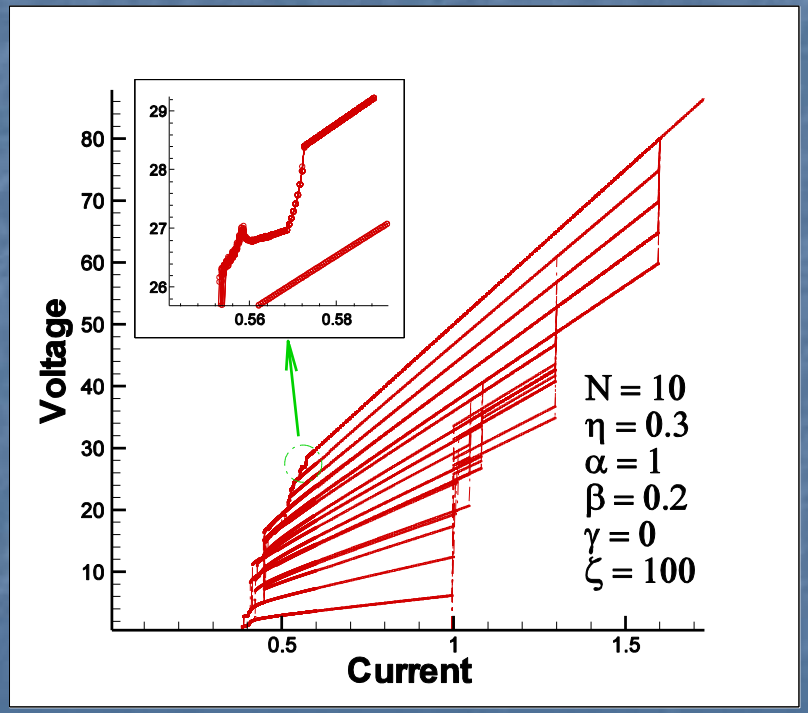

Effect of eta, alpha and beta

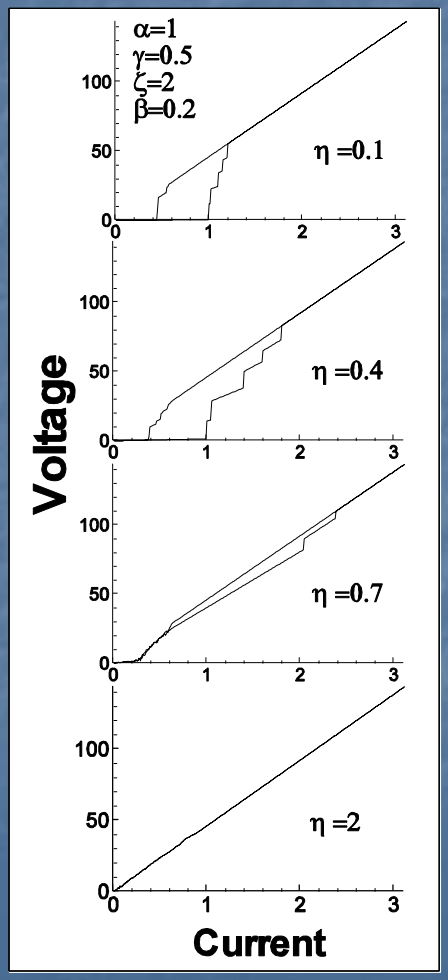

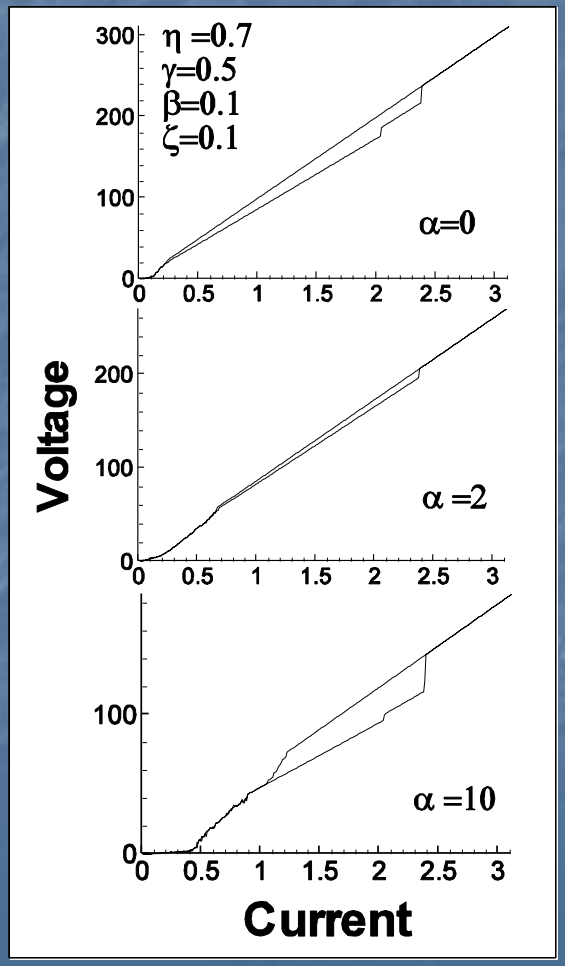

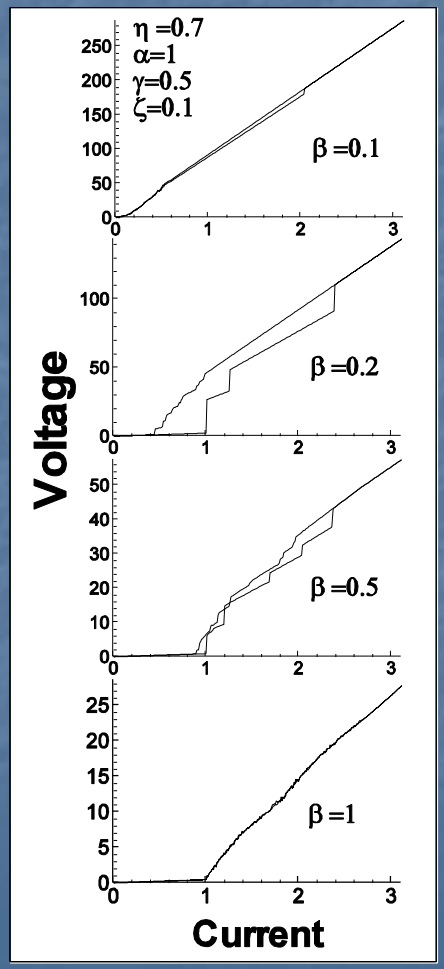

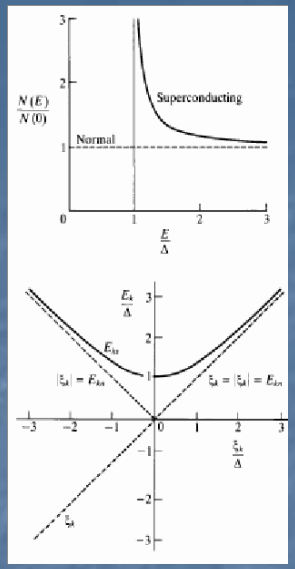

$$\frac{N_s(E)}{N(0)} = \frac{d\xi}{dE} = \begin{cases} \dfrac{E}{(E^2 - \Delta^2)^{1/2}} & (E > \Delta) \\ 0 & (E < \Delta) \end{cases}$$

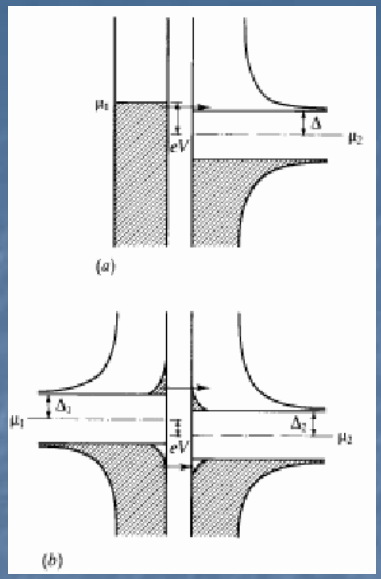

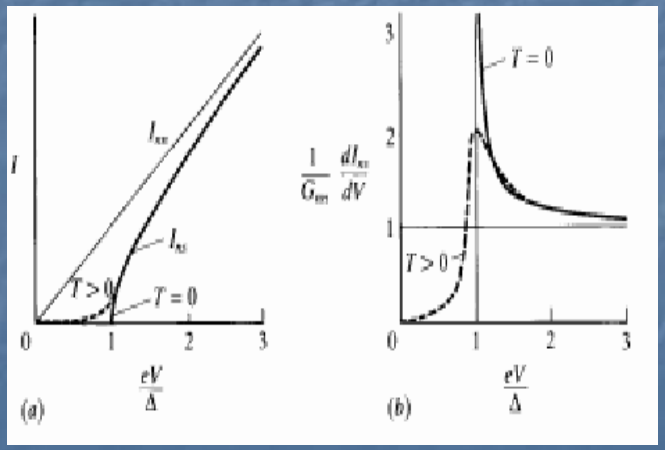

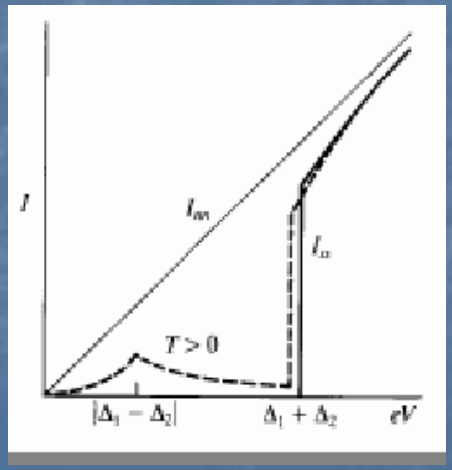

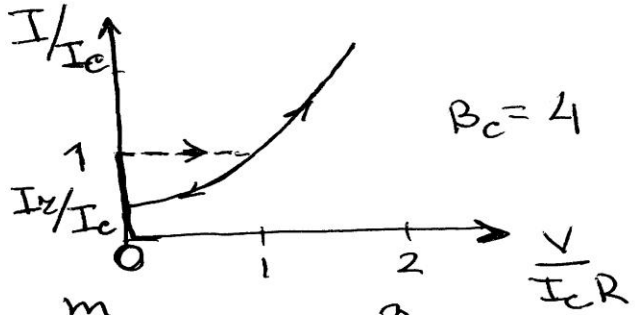

$\beta_c = 4$

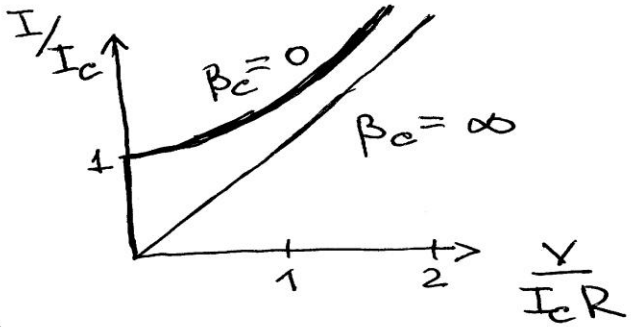

$$\underbrace{\left(\frac{\hbar}{2e}\right)^2 C}_{m}\ddot{\varphi} + \underbrace{\left(\frac{\hbar}{2e}\right)^2 R^{-1}}_{\eta}\dot{\varphi} + \underbrace{E_y}_{E_y(1-\cos\varphi)}\sin\varphi = \underbrace{E_y \frac{I}{I_c}}_{F} \qquad \frac{mv^2}{2} = \frac{CV^2}{2}$$

J - момент инерции

η - вязкость

mgl - макс. грав. момент

Вращ. момент

$$\omega_p = \left(\frac{E_y}{J}\right)^{1/2} \quad - \text{ПЛАЗМ. ЧАСТОТА}$$

$$E = E_y(1-\cos\varphi) - \frac{\Phi_0}{2\pi} I\varphi$$

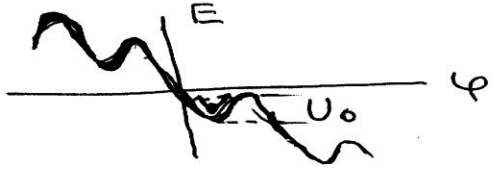

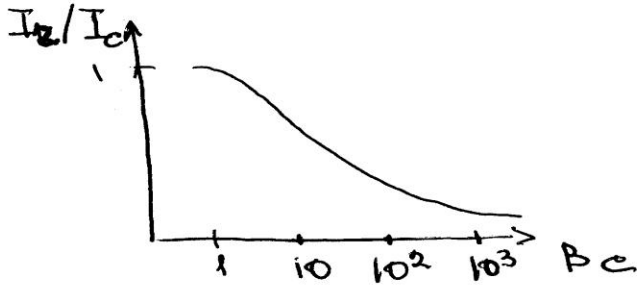

$$\beta_c = \left(\frac{2e}{\hbar}\right) I_c C R^2$$

$$\beta^2 = \frac{1}{\beta_c}$$

Comparison with the experimental results

8 IJJ, $Bi_2Sr_2CaCu_2O_y$, T=77 K, $I_c = 240$ μA.
$\Delta V = 39.1$ mV, $N = 8$ -> $R_n = 20.4$ Ω.
$S = 25\mu m^2$, $d_t = 12$Å, $\varepsilon_r = 10$ -> $C = \varepsilon S/d_t = 1.84$ pF.
Using these data, we can estimate McCumber parameter:
$\beta_c(77\ \mathrm{K}) \approx 560$.
In Zappe model, based on $I_r/I_c = 4/(\pi\beta_c^{-1/2})$ at $\beta_c >> 1$ we get
$I_r \simeq 13$ μA (or $I_r/I_c = 0.054$).
This value is essentially different from the experimental one $I_r = 45$ μA (or $I_r/I_c = 0.188$)
A.Irie, Yu.Shukrinov, G.I.Oya, Appl.Phys.Lett, 93, 152510 (2008)

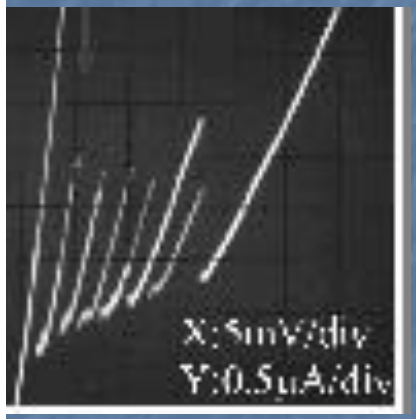

Currents in hysteretic region in CCJJ model

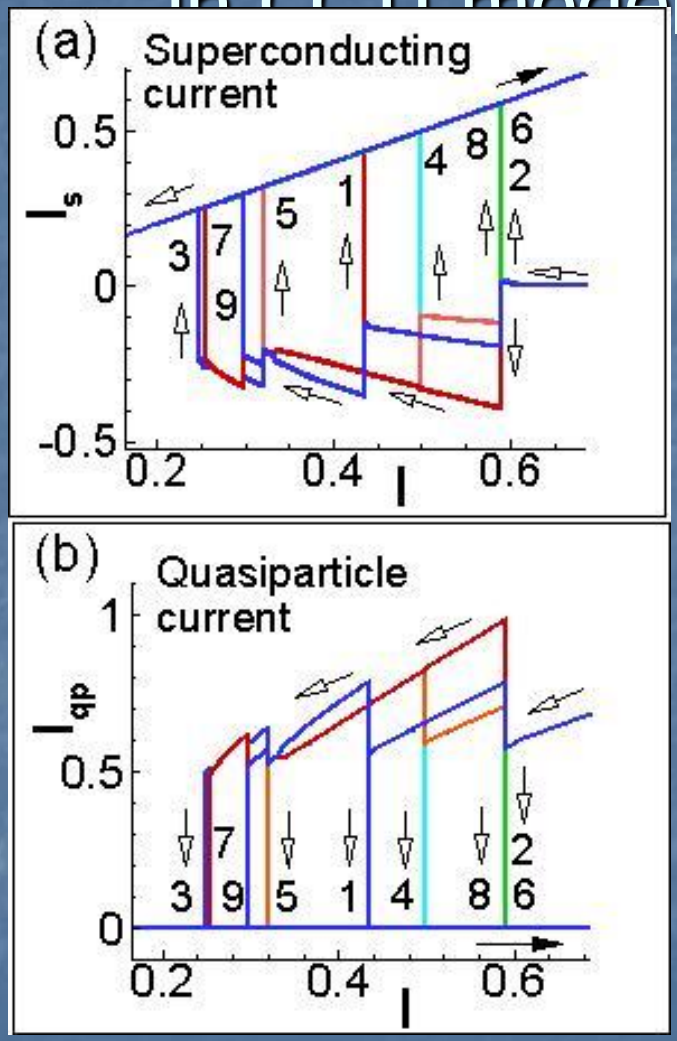

Yu.M.Shukrinov, I.Rahmonov JETP Letters (2010).

Averaged currents in CCJJ+DC model

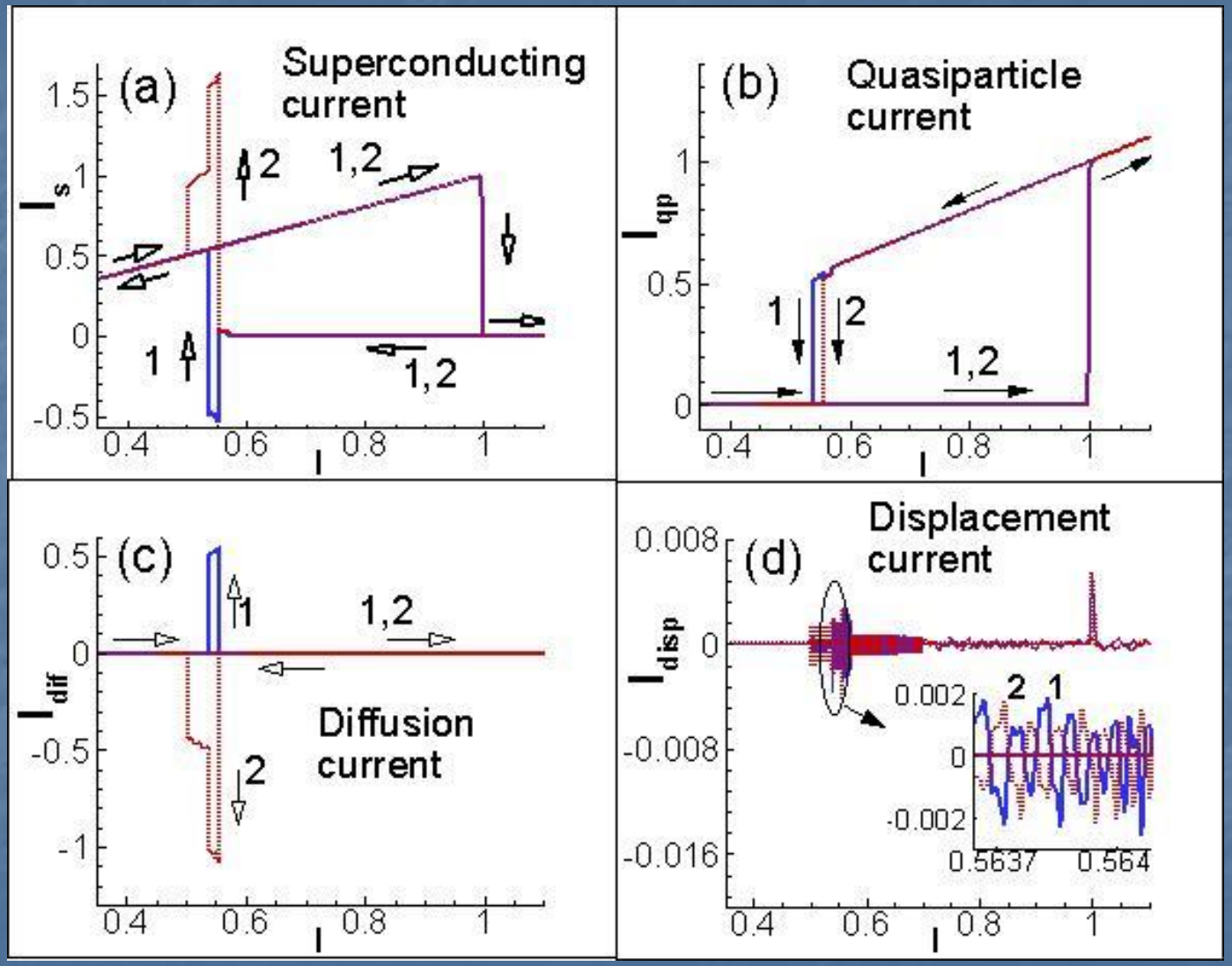

Yu.M.Shukrinov, I.Rahmonov JETP Letters (2010).

CVC in CCJJ and CCJJ+DC models.

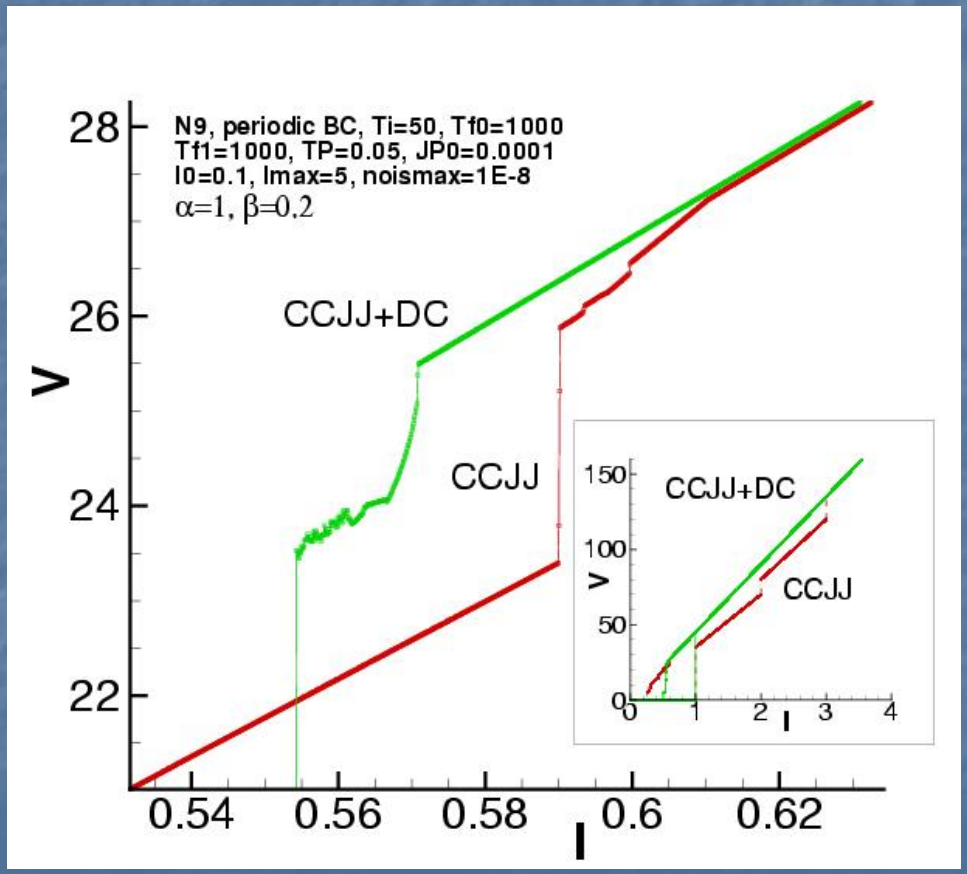

M. Machida, T. Koyama, and M. Tachiki, Phys. Rev. Lett. 83, 4816 (1999).

- Спасибо за внимание